Scientific Reports

https://doi.org/10.1038/s41598-025-30956-9

Article in Press

NMR- and MS-based multiplex approach for comparative metabolome profiling of *Curcuma caesia versus curcuma longa* rhizomes and in relation to in vitro biological effects

Received: 24 August 2025

Accepted: 28 November 2025

Published online: 18 December 2025

Cite this article as: El-Akad R.H., Mohamed T.A., Nicolescu A. *et al.* NMR- and MS-based multiplex approach for comparative metabolome profiling of *Curcuma caesia versus curcuma longa* rhizomes and in relation to in vitro biological effects. *Sci Rep* (2025). https://doi.org/10.1038/s41598-025-30956-9

Radwa H. El-Akad, Tarik A. Mohamed, Alexandru Nicolescu, Teshome Degfie Beshah, Sherif R. Abdel-All, Andrei Mocan & Mohamed A. Farag

NMR- and MS-based Multiplex approach for comparative metabolome profiling of *Curcuma caesia versus Curcuma longa* rhizomes and in relation to *in vitro* biological effects

Radwa H. El-Akad[1], Tarik A. Mohamed[2], Alexandru Nicolescu[3], Teshome Degfie Beshah[4,5], Sherif R. Abdel-All[6], Andrei Mocan[3,7], Mohamed A. Farag[8*]

[1] Pharmacognosy Department, Pharmaceutical and Drug Industries Research Institute, National Research Centre, Cairo P.O. Box 12622, Egypt

[2] Chemistry of Medicinal Plants Department, National Research Centre, 33 El-Bohouth St., Dokki, Giza, 12622, Egypt

[3] Laboratory of Chromatography, Institute of Advanced Horticulture Research of Transylvania, University of Agricultural Sciences and Veterinary Medicine, 3-5 M˘an˘ăștur Street, 400372, Cluj-Napoca, Romania

[4] Department of Chemistry, Adama Science and Technology University, P.O. Box 1888, Adama, Ethiopia

[5] Institute of Pharmaceutical Sciences, Adama Science and Technology University, P.O. Box 1888, Adama, Ethiopia

[6] Department of Pharmacognosy, Faculty of Pharmacy, Alsalam University, Kafr Al Zayat, Al Gharbia, 31611, Egypt

[7] Department of Pharmaceutical Botany, "Iuliu Haţieganu" University of Medicine and Pharmacy, Gheorghe Marinescu Street 23, 400337, Cluj-Napoca, Romania

[8] Pharmacognosy Department, College of Pharmacy, Cairo University, 12613 Cairo, Egypt

***Corresponding authors: mohamed.farag@pharma.cu.edu.eg**

Abstract

The study presents the first integrated comparative metabolomics approach of *Curcuma caesia* known as blue curcuma, that is relatively less explored, compared with the well-known yellow curcuma *Curcuma longa* using a multiplex analytical approach viz., UV, NMR, UPLC/MS/MS, GC/MS and SPME/GC/MS. The study targeted fingerprinting and chemical characterization of their primary and secondary metabolites as well as annotation of volatiles affecting their aroma and culinary uses. Datasets were further modelled using multivariate data analyses (PCA and OPLS) for samples' classification and discrimination. The study revealed several newly reported metabolites in blue curcuma and assigned discriminating biomarkers for each species i.e. sesquiterpenes in blue curcuma *vs* curcuminoids in yellow curcuma. Bioactivity assays, including antioxidant and antidiabetic activities, showed moderate activity for *C. caesia* relative to *C. longa,* while both species were inactive as anti-obesity agents.

Keywords: Blue Curcuma, *C. caesia*, *C. longa*, metabolites profiling, UPLC/MS/MS, GC/MS, NMR

1- Introduction

Curcuma is a prominent genus in the family Zingiberacea that comprises ~100 species; globally recognized for their applications in traditional medicine, culinary arts, food industry, therapeutic products, cosmetics, as well as sources for natural pigments [1,2]. Despite being native to tropical and subtropical areas in Asia, the word "*Curcuma"* is originally derived from the Arabic word "kurkum" which means "yellow" referring to the rhizome color [2,3].

Curcuma longa, known as yellow turmeric, is the most notable species that has a long ethnobotanical history in Ayruvedic and Unani medicine and reported for wide array of pharmacological activities attributed to its enriched phytochemical reservoir viz. curcuminoids, aroma compounds, and polyphenols [2-4]. In contrast, *C. caesia,* known as blue/black turmeric after its distinguished rhizome color, remains relatively less explored despite being traditionally used for the treatment of various ailments including gastrointestinal tract disorders, wound healing, respiratory disorders, fever, rheumatoid arthritis, among several others [5,6]. Previous phytochemical studies reported sesquiterpenes, flavonoids and volatile constituents in blue curcuma as well as positively reacting to screening assays for alkaloids, tannins and phenolics [5,7-9]. Both species are reported to have significant pharmacological activity against cancer, inflammation, bacterial and fungal infections, liver diseases, and other metabolic disorders [2,3,5,6,8].

Despite extensive studies on *C. longa* and increasing interest in *C. caesia,* an integrated and comprehensive comparative study between both species has yet to be performed that aids provide deeper insight on the metabolome of blue curcuma, in particular. This study presents the first multiplex analytical approach for a complementary metabolomics overview of both blue and yellow curcuma, using fingerprinting techniques i.e., ultraviolet absorbance (UV), nuclear magnetic resonance (NMR), versus hyphenated techniques i.e., ultra-performance liquid chromatography coupled to high resolution mass spectrometry (UPLC/HR-MS/MS), gas chromatography coupled to mass

spectrometry (GC/MS) and solid phase microextraction-(SPME-GC/MS). The multi-platform metabolomic analyses presented in this study offer untargeted chemical characterization of polar, semi-polar and non-polar metabolites in addition to volatile constituents. Multivariate data analyses including principal component analysis (PCA) and orthogonal partial least squares discriminant analysis (OPLS-DA) were employed to classify among samples and biomarker assignment. Furthermore, antioxidant activity was investigated using different assays i.e. 1,1-diphenyl-2-picrylhydrazyl (DPPH), 2,2'-azino-bis(3-ethylbenzothiazoline) 6-sulfonic acid (ABTS) and ferric reducing antioxidant power (FRAP) to assess their free radical scavenging activity comparatively, alongside quantification of their total phenolic and flavonoid content. Further, *in vitro* assay of both turmeric samples against glucosidase and lipase enzymes was investigated as a marker for diabetes or obesity management.

2- Material and Methods

2.1. Plant material

C. caesia and *C. longa* were collected from Chongzuo, Guangxi Province, during the winter of 2023. Dr. Kai Wang authenticated rhizomes at the Chinese Academy of Sciences, Beijing. Rhizomes were lyophilized overnight and stored in sealed containers until further assays. Specimen was deposited at the herbarium of Faculty of Pharmacy-Cairo University, voucher no.: 1-12-23-F.

2.2. UV fingerprinting of C. caesia and C. longa chloroform extracts

Three grams of each freeze-dried powdered *Curcuma* sample was macerated with 30 mL chloroform for 2 h, then centrifuged and filtered. An aliquot of 200 µL was used, prepared from four replicates in a 96-well plate for the Gen 5 Greener UV microplate reader (Gen 5, kitted with a 96-well quartz cell with 1 nm spectral resolution in the UV region). Aliquots of each curcuma extract (200 µL) were pipetted into the microplate wells (n = 4) of a Gen 5 Greener UV microplate quartz reader (BioTek Instruments, Inc., Winooski, VT, USA). The absorption spectra were recorded in the range of 200–500 nm [10]

2.3. NMR fingerprinting of C. caesia and C. longa methanol extracts

Five milliliters of the methanol extract were aliquoted and subjected to drying under a nitrogen stream till complete dryness, and pellet was further resuspended in 700 ul CD_3OD containing 0.96 mM hexamethyldisilane (HMDS) as an internal standard. All spectra were obtained using a Varian/Agilent VNMRS 600 NMR spectrometer, operating at proton and carbon NMR frequencies of 599.83 MHz and 150.84 MHz, respectively, with a 5-mm inverse detection cryoprobe. The ^1H NMR spectra were recorded with a spectral resolution of 0.26 Hz/point (Spectral Width, SW = 8389 Hz, acquisition size = 64 K complex points, zero-filled to a final Fourier transform (FT) size of 128 K). The parameters used were as follows: pulse width (pw) = 6 µs (90°), relaxation delay = 22.3 s, acquisition time = 2.7 s, and 120 scans [11,12].

HMBC spectra were acquired with a bandwidth of 14 ppm in F2 (^{1}H) and 235 ppm in F1 (^{13}C), using two scans per 256 increments for F1 and 2516 complex data points in F2. The HMBC experiments were optimized for long-range couplings of 8 Hz, with a relaxation delay of 1 s and an acquisition time of 0.15 s, resulting in a total acquisition time of 22 min. To minimize degradation and artifact formation, all NMR spectra were recorded from samples prepared immediately before data acquisition, within a 6-h time frame. Spectra were automatically phase-corrected, with proton and carbon chemical shifts referenced to TSP at (δ1H = 0.0 ppm) and internal CD_3OD (δ13C = 49.86 ppm), respectively [11,12].

Additionally, 2D-NMR spectra, including ^{1}H single bond^{1}H total correlation spectroscopy (TOCSY), ^{1}Hsingle bond ^{13}C heteronuclear single-quantum coherence (HSQC), and ^{1}H single bond ^{13}C HMBC, were recorded for selected samples using standard CHEMPACK 7.1 pulse sequences (zTOCSY, gHSQCAD, and gHMBCAD) implemented in the Varian VNMRJ 4.2 A spectrometer software.

2.4. NMR Quantification

For metabolites quantification using NMR spectroscopy, the peak areas of selected proton signals belonging to the target compounds and the internal standard (TSP) were integrated manually for all samples [11]. The following equation was applied for absolute metabolite level calculations [13]:

$$m_T = M_T \, X \, (I_T/I_{St}) \, X \, (X_{St}/X_T) \, X \, C_{St} \, X \, V_{St}$$

m_T: mass of the target compound [µg/g] in the solution used for ^{1}H NMR measurement.

M_T: molecular weight of the target compound [g/mol].

I_T: relative integral value of the ^{1}H NMR signal of the target compound.

I_{St}: relative integral value of the ^{1}H NMR signal of the standard compound.

X_{St}: number of protons belonging to the ^{1}H NMR signal of the standard compound.

X_T: number of protons belonging to the ^{1}H NMR signal of the target compound.

148 C_{St}: concentration of internal standard (TSP) in the solution used for ^{1}H NMR
149 measurement [mmol/L].
150 V_{St}: volume of solution used for ^{1}H NMR measurement [mL]

151 *2.5. Metabolites profiling of C. caesia and C. longa extracts via UPLC/HR-*
152 *MS/MS*

153 Briefly, 150 mg of each *Curcuma* fine powder specimen was homogenized
154 with 5 mL MeOH (100% *v/v*) containing 10 µg/mL umbelliferone as an internal
155 standard using an Ultra-Turrax mixer (IKA, Staufen, Germany) adjusted at
156 11,000 rpm, five times for 20 s periods, with intervals of 1 min between each
157 mixing period to guard against temperature increases and heating effects. The
158 resultant suspensions were then vortexed vigorously, centrifuged at
159 3000× *g* for 30 min, and filtered through a 22 µm pore size filter to remove
160 plant debris. Then, 1 mL was aliquoted and filtered, and placed in LCMS vials
161 [10]. Three independent replicates (n = 3) were done for each sample to assess
162 biological variance.

163 The principal step of UPLC/HR-MS/MS analysis was conducted in triplicate
164 (*n* = 3), with 2 µL introduced to an Dionex 3000 UPLC system (Thermo Fisher
165 Scientific, Bremen, Germany) equipped with a HSS T3 column (100 × 1.0 mm,
166 1.8 µm; Waters®; column temperature: 40 °C), and a photodiode array detector
167 (PDA, Thermo Fisher Scientific, Bremen). Binary gradient elution protocol at a
168 flow rate of 150 µL/min using water/formic acid, 99.9/0.1 (*v/v*) (A) and
169 acetonitrile/formic acid 99.9/0.1 (*v/v*) (B) varying between isocratic step for 1
170 min of 5% mobile phase B, then a linear increase of B from 5% to 100% over
171 11 min. The mobile phase was kept isocratic between 11–19 min at 100% B
172 followed by decreasing towards 5% B within 1 min, and, finally, an additional
173 10 min, i.e., 20–30 min, for column re-equilibration using 5% B[10] .

174 The UPLC system was coupled with a high-resolution mass spectrometer
175 using an Orbitrap Elite mass spectrometer (Thermo Fisher Scientific, Bremen,
176 Germany) equipped with a HESI electrospray ion source (spray voltage:
177 positive ion mode 4 kV, negative ion mode 3 kV; source heater temperature:

250 °C; capillary temperature: 300 °C; FTMS resolution: 30,000). Nitrogen was used as sheath and auxiliary gas. The CID mass spectra (buffer gas: helium; FTMS resolution: 15,000) were recorded in data-dependent acquisition mode (dda) using a normalized collision energy (NCE) of 35% and 45% [14].

2.6. GC/MS analysis of silylated primary metabolites in C. caesia and C. longa

Briefly, finely powdered samples (100 mg) were extracted with 5 mL 100% methanol, aided by sonication and for 30 min at room temperature using Branson CPX-952-518R (Branson Ultrasonics, Carouge, SA Switzerland). The extracts were then centrifuged (LC-04 C 80-2 C regen lab centrifuge, Zhejiang, China) at 12,000× g for 10 min. Three independent replicates (n = 3) were done for each sample to assess biological variance.

Then, 100 µL of the methanol extract was evaporated to dryness in opened screw-cap vials by using stream of nitrogen gas. For derivatization, 150 µL of N-methyl-N-(trimethylsilyl)-trifluoroacetamide (MSTFA) previously mixed (1:1) with anhydrous pyridine was added to the dried methanol extract and the mixture was incubated (Yamato Scientific DGS400 Oven, QTE TECHNOLOGIES, Hanoi, Vietnam) for 45 min at 60 °C. Silylated derivatives were separated on a Rtx-5MS Restek, Bellefonte, PA, USA (30-m length, 0.25-mm inner diameter and 0.25-m film). [14,15].

2.7. SPME-GC/MS analysis of volatile constituents in C. caesia and C. longa

Briefly, 20 mg of finely pulverized powder were placed in 1.5 ml SPME screw-cap vials quickly sealed and set on a tray that was kept at a constant 50 °C for 30 min. During that time, SPME fibers of stable flex coated with divinylbenzene/carboxen/polydimethylsiloxane (DVB/CAR/PDMS) 1 cm long of 50/30 µm purchased from Supelco® (Oakville, ON, Canada) were used for sampling by incubation in the headspace above the sample. The analysis of volatile compounds was carried out on a Schimadzu® GC-17 A gas chromatograph equipped with a DB-5 column (30 m x 0.25 mm i.d. x 0.25 µm

film thickness; Supelco) and coupled to Schimadzu® QP5050A mass spectrometer [14,15].

2.8. Multivariate data analyses

Both UPLC/MS/MS and GC-MS derived datasets for primary and secondary metabolites were subjected to unsupervised PCA and supervised OPLS-DA multivariate data analysis using SIMCA-P version 14.1 software package (Umetrics, Umeå, Sweden). All variables were mean-centered and scaled to Pareto variance. Unsupervised PCA was used to obtain a segregation pattern of the variance of metabolites among the samples. While the supervised OPLS-DA was used to verify PCA results, identify markers, and obtain detailed information on the distinctions among the studied specimens. The Chemometric models with several permutations were applied for models' validation based on the main 2 indices, including R^2 and Q^2. Model predictability was indicated by Q^2, and model goodness of fit was specified by R^2 [10,15].

2.9. Quantification of total phenolic (TPC) and flavonoid contents (TFC)

The TPC and TFC in rhizome methanolic extract of *C. caesia* and *C. longa* were analyzed using 96-well plates with a SPECTROstar® Nano Multi-Detection Microplate Reader (BMG Labtech, Ortenberg, Germany) following Folin-Ciocâlteu assay for TPC and aluminium chloride ($AlCl_3$) colorimetric assay for TFC [16,17].

In detail, for TPC determination: 20µl extract (2.0 mg/mL) was mixed with 100 µL Folin-Ciocâlteu reagent, and 80 µL sodium carbonate (7.5% *w/v*) ad incubated for 30 min at room temperature followed by measuring the absorbance at 760 nm using gallic acid as reference drug (0.011–0.154 mg/mL, R^2=0.99). Results are expressed as mean of triplicates (n=3) ± S.D as gallic acid equivalent per gram of freeze-dried powder (GAE/g w).

For TFC determination: the absorbance of the mixture constituted of 40 µL extract (2.0 mg/mL), 40 µL sodium acetate (100 mg/mL) and 24 µL

$AlCl_3$ (25 mg/mL) in ethanol (total volume 200 µL) was measured at 430 nm (n=3). Results were expressed as mean ± S.D. rutin equivalent per gram of freeze-dried powder (RE/g w). Calibration curve constructed of rutin at concentration range 0.025–0.125 mg/mL (R^2=0.99)

2.10. Bioactivity assays

2.10.1. Antioxidant activity determination [16]

2.10.1.1. DPPH assay

The assay was conducted following the same procedures described by Zayed et al.,[16,18]. Mixture of 30 µL extract and 270 µL 0.004% DPPH in methanol was incubated for 30 min. in darkness at room temperature followed by measuring its absorbance at 515 nm (n=3). Results are expressed as mean ± S.D. mg trolox equivalent/ gram weight of dried residue (mg TE/g w).

2.10.1.2. ABTS assay

The assay followed the exact procedures mentioned by Zayed et al., [16,18]. The absorbance of the extract (2 mg/mL) and ABTS solution mixture was measured at 734 nm upon 30 min incubation at room temperature (n=3). Results are expressed as mean ± S.D. mg trolox equivalent/ gram weight of dried residue (mg TE/g w) [18,19].

2.10.1.3. FRAP assay

The assay was performed as described by Zayed et al., [16,18]. The absorbance of 20 µL extract (2 mg/mL) and 175 µL FRAP reagent mixture was measured at 593 nm upon 30 min. incubation at room temperature (n=3). Results are expressed as mean ± S.D. mg trolox equivalent/ gram weight of dried residue (mg TE/g w)

2.10.2. Antidiabetic activity determination via α-glucosidase inhibition

The assay followed exact protocol in Zayed et al., [18,20]. The mixture of extract (0.1–2 mg/mL), substrate, phosphate buffer, and yeast *α*-glucosidase was incubated at 37°C before measuring the absorbance of the obtained color

at 405 nm against blank and acarbose reference drug. % of Inhibition was calculated according to the following equation:

$$\% \text{ of Inhibition} = 100 \text{ X} \quad \frac{\text{Abs}_{\text{(control)}} - \text{Abs}_{\text{(Sample)}}}{\text{Abs}_{\text{(control)}}}$$

The normalized logarithmic curve for % inhibition was used to express the data as IC_{50}±SD (the concentration of the sample that could inhibit 50% of the enzyme for triplicates, n = 3).

2.10.3. Anti-obesity assay determination via lipase inhibition

The assay was proceeded exactly as described by Zayed et al., [18]. The crude porcine PL type II at 2.5 mg/mL (Sigma, EC 3.1.1.3) was suspended in 5 mM Tris–HCl buffer (pH 8.0, obtained using HCl). The mixture was centrifuged (6987.5×*g*, 8 min, 20.0 ± 1.0 °C), and the clear supernatant was isolated. Afterward, 40 µL of PL solution were pre-incubated for 15 min at 37 °C with 40 µL of varying concentrations (0.25–10 mg/mL) of each extract, then 4-nitrophenyl butyrate (*p*-NPB) substrate at a concentration of 10 mM in pure ethanol was added. The absorbance was measured spectrophotometrically at 405 nm in microplates, after another 5 min of incubation. Orlistat was used as a positive drug control for the assay [18,21]

3- Results and Discussion

3.1. UV fingerprinting of *C. caesia* and *C. longa* extracts

Considering the clear color difference in both rhizome pulps that is blue versus yellowish, UV fingerprinting was employed initially for identification of the nature of coloring matter in blue curcuma. Blue curcuma was investigated for the presence of azulenes (conjugated 5- and 7-membered fused ring system) that is known to impart bluish coloration. Due to its non-polar nature, and lower solubility in methanol, extraction was attempted with chloroform for both yellow and blue curcuma rhizome powder for comparative analysis (**Suppl. Fig. S1**). Extraction using methanol failed to show absorbance spectra for these phytochemicals. From literature, azulenes show maximum absorbance at λ_{max} 270-340 nm (< 350 nm) that corresponds to $S_0 \rightarrow S_2$ transition (short wavelength) [22], whereas, in this study blue curcuma showed an exclusive strong absorbance at longer wavelength ca. λ_{max} 400 nm, that inferred the presence of guaiazulenes (alkylated derivatives of azulenes) [23]. Guaiazulenes are lipophilic bicyclic sesquiterpene hydrocarbons having distinctive bluish-purple color and common in planta [23,24]. The alkyl substitution in guaiazulenes viz. methyl and isopropyl moieties; donates electrons to the conjugated ring π- system, thus, reduces the gap between the highest occupied molecular orbital (HOMO) and the lowest unoccupied molecular orbital (LUMO) i.e. ground and excited states, which in turn causes bathochromic shift in ($S_0 \rightarrow S_1$) and ($S_0 \rightarrow S_2$) absorption [22,24-26].

3.2. NMR fingerprinting of *C. caesia* and *C. longa* methanol extracts

NMR analysis was performed on *C. caesia* and *C. longa* extracts to elucidate major metabolites differences and also aided in standardization for quality control. Leveraging prior NMR-based literature, peaks corresponding to major metabolites in *C. caesia* (BT) and *C. longa* (YT) were identified. As summarized in **Table 1**, a diverse array of metabolites was classified into three major phytochemical groups, comprising 11 chemically distinct compounds: 5

sesquiterpenes (1–5), 3 curcuminoids (6–8), and 3 primary metabolites (9–11). The identified metabolites are shown in **Suppl. Fig. S2.**

3.2.1. Sesquiterpenes

Sesquiterpenes (15-carbon terpenoids) represent a structurally diverse class of secondary metabolites. Curdione, exclusive to *C. caesia*, displays three methyl doublets (CH_3-13 at δ_H 0.84, J = 6.6 Hz; CH_3-12 and CH_3-14 at δ δ_H 0.94), confirming its germacrane skeleton. Key HMBC correlations from CH_3-14 to the ketone C-5 (δ_C 216.6) validate ring fusion [27,28]. Xanthorrhizol, present in both species, exhibits a trisubstituted olefin (H-12, δ_H 5.34) and characteristic methyl signals: a doublet (CH_3-9, δ_H 1.17, J = 3.0 Hz) and singlets (allylic CH_3-14/15, δ_H 1.81; vinylic CH_3-7, δ_H 2.07). HMBC correlations link CH_3-7 to olefinic C-2 (δ_C 123.2) and C-3 (δ_C 139.5), confirming its bisabolane core [29,30]. Furanodienone (both species) features a furan ring evidenced by H-5 (δ_H 5.87, s) and methyl groups (H-13, δ_H 2.06; H-14, δ_H 1.94, d, J = 1.2 Hz), with HMBC correlating H-14 to furan carbons C-3 (δ_C 41.0), C-4 (δ_C 147.7) and C-5 (δ_C 133.2) (Oon et al., 2016). Curcuzederone (both species) showed a phenolic structure with an aromatic proton (H-12, δ_H 7.16, s) and methoxy group (H-5, δ_H 3.74, s). Curcuminol G, exclusive to *C. caesia*, is identified by three methyl singlets (H-13–H-15, δ_H 1.09–1.87) and an HMBC correlation from H-13 to a carbonyl (C-12, δ_C 180.0), suggesting a sesquiterpenoid acid/ester (**Fig. 1A , 1B, Suppl. Fig. S3 and S4, Table 1**) [27-32].

3.2.2. Curcuminoids

Curcuminoids, diarylheptanoid pigments exclusive to *C. longa*, share diagnostic *trans*-olefinic protons: H-3/H-3′ (δ_H 6.59, d, J = 15.8 Hz) and H-4/H-4′ (δ_H 7.55, d, J = 15.8 Hz), confirming the conjugated diene system (Khattab et al., 2022). Curcumin I displays asymmetric *meta*-substituted aromatics: H-6/H-6′ (δ_H 7.20, d, J = 1.7 Hz) and H-10/H-10′ (δ_H 7.09, dd, J = 8.6, 1.7 Hz). Curcumin II shows mixed substitution: one ring with *meta*-coupling (H-6, δ_H

7.20) and the other with *ortho*-coupling (H-6′/H-10′, δ_H 7.47, d, J = 8.6 Hz; H-7′/H-9′, δ_H 6.80, d, J = 8.6 Hz). Curcumin III exhibits symmetric *ortho*-substitution: equivalent aromatic protons for both rings (H-6/H-10 & H-6′/H-10′ at δ_H 7.47; H-7/H-9 & H-7′/H-9′ at δ_H 6.79). Their absence in *C. caesia* explains its lack of yellow pigmentation (**Fig. 1C, Table 1**) [27,33,34].

3.2.3. Primary Metabolites

Primary metabolites, conserved in both species, reflect essential cellular functions, and moreover nutritive value in both rhizomes. Methionine was identified by its sulfur-methyl group (S-CH_3, δ_H 2.07, s) and α-methine proton (NH_2-CH, δ_H 3.30, m), with HMBC correlating S-CH_3 to β-methylene (δ_C 29.9) (Wang et al., 2015). Choline showed a sharp singlet for its trimethylammonium group [$N(CH_3)_3$, δ 3.18, s]. Fumaric acid exhibits a broad singlet (δ_H 6.64) for its equivalent olefinic protons (CH=CH), consistent with its symmetric *trans*-structure. These compounds underpin universal metabolic roles: methionine in methylation, choline in membrane integrity, and fumaric acid in the Krebs cycle (**Fig. 1A and 1B, Table 1**) [27,30,31].

Quantitative ^{1}H-NMR analysis of key metabolites in *C. caesia* (BT), and *C. longa* (YT).

^{1}H-NMR (qNMR) was employed to determine the absolute concentrations (µg/g) of key metabolites (7 metabolites out of 11 identified metabolites) underscores profound metabolic divergence between *C. caesia* (BT) and *C. longa* (YT), revealing species-specific biochemical strategies (**Suppl.Table S1**) BT's exclusive production of curdione (1.1 µg/g, germacrane-type) and furanodienone (1.4 µg/g, furanosesquiterpenoid) aligns with its traditional use in anti-inflammatory therapies, while the absence of these in YT highlights evolutionary pathway specialization [35]. Conversely, xanthorrhizol is more abundant in BT (1.5 µg/g) than in YT (1.4 µg/g; bisabolane-type), whereas YT's exclusive accumulation of curcumin I (0.93 µg/g) directly correlates with its antioxidant and iconic pigmentation absent in BT due to silenced

diarylheptanoid biosynthesis (Jantan et al., 2012). Notably, Curcuzederone exhibits preferential accumulation in BT (0.9 µg/g vs. 0.3 µg/g in YT), suggesting differential regulation of phenolic sesquiterpenoid pathways, whereas near-identical curcuminol G levels (0.3 µg/g BT vs. 0.1 µg/g YT) imply conserved enzymatic machinery for this sesquiterpenoid acid. The exclusive detection of choline in BT (0.1 µg/g) further indicates distinct primary metabolism, potentially supporting membrane biosynthesis in stress adaptation. These quantified disparities rooted in proton-specific integrals (e.g., 3H for methyl groups vs. 1H for olefinics) provide not only chemotaxonomic markers for species authentication but also a biochemical rationale for their ethnopharmacological differentiation, with BT as a sesquiterpene-rich analgesic, and YT as a curcuminoid-centric antioxidant[36-38].

3.3. Metabolites profiling of *C. caesia* (BT) and *C. longa* (YT) rhizome methanol extracts *via* UPLC/HR-MS/MS analysis in both ionization modes

Metabolites profiling of BT and YT *via* UPLC/HR-MS/MS analysis in both negative and positive modes provided improved secondary metabolites coverage for less abundant secondary metabolites not detected using NMR [39]. Gradient system of water (0.1% formic acid): acetonitrile eluted metabolites from the most to the least polar throughout a 20 min. runtime. Annotation of metabolites was based on MS data, including molecular ion, product ions, respective elemental formulae (error< 5 ppm), and fragmentation pattern; in accordance with previously published literature and databases e.g., Reaxys , HMDB, FooDB, Pubchem, and phytochemical dictionary of natural products, in addition to predicted spectra generated by CFM-ID (https://cfmid.wishartlab.com). Base peak chromatograms (BPC) of *Curcuma* sp. in both modes are shown in **Figure 2**. The identified metabolites are listed in **Table 2** based on their classes. Structures of selected metabolites annotated in both species are demonstrated in **Figure 3**.

Overall, UPLC/MS analysis revealed 110 metabolites including 7 sugars, 4 organic acids, 10 phenolics, 5 cinnamates, 5 flavonoids, 1 anthocyanin, 2 alkaloids, 23 di/aryl alkanoids, 24 sesquiterpenes, 21 fatty acids/glycerolipids, and 8 miscellaneous compounds (**Table 2**). Common fragmentation pathways in MS/MS spectra included dehydration (-H_2O, 18 amu), deglycosilation (-$C_6H_{10}O_5$, 162 amu for hexose, $C_5H_8O_4$, 132 amu for pentose, -$C_6H_{10}O_4$, 146 amu for deoxyhexose), decarboxylation (-COO, 44 amu), demethoxylation (-OCH_3, 30 amu), decarbonylation (-CO, 28 amu), dealkylation, retro-Diels-Alder (RDA), and ring cleavage, as discussed in detail in the next subsections. UPLC/HR-MS/MS analysis provided insight into the chemical reservoir of *C. caesia* with several detected metabolites are reported herein for the first time, and adding to that taxa rich chemical composition.

3.1. Organic acids

Low molecular weight organic acids play a role in rhizomes to alleviate microbial stress and reduce heavy metals absorption [40]. Herein, 4 organic acids were detected in blue curcuma, *viz.* malic, citric, succinic and benzoic acids in peaks 1-4 early eluted at Rt range 0.9-1.7 min (**Table 2**) [4]. Observed fragments included decarboxylated and dehydrated product ions matching databases. For example, citric acid [M-H]$^-$191.01881, $C_6H_7O_7^-$ showed dehydrated ion at *m/z* 173, $C_6H_5O_6^-$, followed by decarboxylation at *m/z* 129, $C_5H_5O_4^-$, and further fragments at *m/z* 111, *m/z* 103, and *m/z* 87.

3.2. Phenolics, flavonoids, and anthocyanins

Phenolics alongside flavonoids are biosynthesized in plants as secondary metabolites mainly to filter or screen ultraviolet rays, alleviating its harmful oxidative stress, and as attractants for pollinators; thus, their abundance in rhizomes is limited relative to leaves [41]. In *Curcuma,* only 14 flavonoids were previously reported [2]. As shown in **Table 2**, 10 phenolics, 3 flavonoids, and 1 anthocyanin were annotated in *C. caesia* versus 3 phenolics and 3 flavonoids in *C. longa;* matching references reported on genus *Curcuma* [3,6,42].

Interestingly, a *p*-hydroquinone derivative was detected exclusively in *C. caesia,* peak 16, at [M-H]$^-$ 331.10275, $C_{14}H_{19}O_9^-$ for the first time (**Table 2**). Such compounds are potent ferric-ion reductants to its GIT-absorbable ferrous form, decolorizing agents, skin lightening agents , anti-inflammatory and potent free radical scavengers [43-47]. Fragmentation pathways yielded deglycosilated product ion at *m/z*168, $C_8H_8O_4^-$, followed by sequential demethylation at *m/z* 153, $C_7H_5O_4^-$ and *m/z* 138, $C_6H_2O_4^-$, further fragments at *m/z* 125, *m/z* 97, *m/z* 93, *m/z* 83, *m/z* 71 and *m/z* 59 corresponding to dehydroxylation and hydroquinone ring cleavage, matching the spectrum of leonuriside A, that is dimethoxy-hydroquinone-*O*-hexoside (**Suppl.Fig.S5**), as reported in literature and databases [48].

Flavans and flavanones were major flavonoid subclasses detected in *C. caesia* in peaks 22, 25 and 26, whereas, *C. longa* had additional flavonols in peaks 22, 24 and 27 (**Table 2**) [2,42]. Pinocembrin flavanone in peak 27 was annotated herein in *C. longa* extract only at [M-H]$^-$ 255.0654, $C_{15}H_{11}O_4^-$, known to exert several health benefits [49,50].

In contrast, malvidin-*O*-rutinoside, detected in peak 23 exclusively in *C. caesia* for the first time, is an anthocyanin that imparts violet color and was previously reported in *C. alismatifolia* pink bracts [2], and could contribute to the blue coloration of *C. caesia* alongside azulenes (**Suppl.Fig.S1**). The molecular ion was detected only in positive ionization mode at [M+H]$^+$ 639.19128, $C_{29}H_{35}O_{16}^+$ (**Suppl. Fig. S6**), which yielded fragments at *m/z* 493, $C_{23}H_{25}O_{12}^+$ and *m/z* 331, $C_{17}H_{15}O_7^+$ for the sequential deglycosilation of deoxyhexose and hexose sugars, respectively, followed by RDA fragmentation of malvidin at *m/z* 153 [51] (**Table 2**).

3.3.3. Cinnamates

In this study, 5 cinnamic acid derivatives were detected in peaks 28-32 (**Table 2**). MS/MS Spectra in peaks 28, 31 and 32 showed feruloyl fragment ion at *m/z* 193, $C_{10}H_9O_4^-$, while peaks 29 and 30 had molecular ion at [M-H]$^-$

179.0335, $C_9H_7O_4^-$ and [M-H]$^-$ 147.04379, $C_9H_7O_2^-$, identified as caffeic and cinnamic acids, respectively. Likewise, ferulic acid derivative in peak 31 annotated as feruloyloxy-methoxycinnamic acid at [M-H]$^-$339.0862, $C_{19}H_{15}O_6^-$, was previously reported in *Curcuma* but first time in *C. longa* rhizome [6]. Another feruloyl derivative in peak 32 in *C. caesia* was annotated as oxyprenylated derivative of ferulic acid, namely, methylbutenoxy-ferulic acid, reported for the first time in *Curcuma* taxa. In detail, molecular ion was detected at [M-H]$^-$ 261.1124, $C_{15}H_{17}O_4^-$ that yielded upon fragmentation several product ions viz. decarboxylated ion at *m/z* 217, $C_{14}H_{17}O_2^-$, feruloyl moiety at *m/z* 193, $C_{10}H_9O_4^-$ upon the loss of the prenyl side chain (C_5H_8), *m/z* 149 $C_9H_9O_2^-$ (-OCH_3 & loss of oxyprenyl sidechain), *m/z* 121, $C_8H_9O^-$ and *m/z* 105 $C_8H_9^-$ (-CO_2, -OCH_3 &loss of pentenyl side chain) followed by dealkylation at *m/z* 79, $C_6H_7^-$ whereas, the isopentenyl side chain was detected at *m/z* 81, $C_5H_5O^-$ and its dealkylated fragment at *m/z* 67, $C_4H_3O^-$ (**Table 1, Suppl.Fig.S7**).

3.4. Alkaloids

In previous studies, *C. longa* was reported to yield hydroxyquinoline alkaloids [2,6]. Herein, 2 hydroxyquinoline alkaloids are reported for the first time in both blue and yellow curcuma as shown in peaks 33 and 34 at [M-H]$^-$ 366.0824, $C_{16}H_{16}NO_9^-$ and [M-H]$^-$ 382.0771, $C_{16}H_{16}NO_{10}^-$annotated as di- and tri-hydroxyquinoline carboxylic acid-*O*-hexoside, respectively (**Table 2**). Fragments aiding in identification included deglycosilation (-162 amu, $C_6H_{10}O_5$), decarboxylation (-44 amu, CO_2) and quinoline ring cleavage matching spectra on databases [52] (**Suppl.Fig.S8**). Similar structures were reported previously in *Ephedra* and cereals to which beneficial health promoting effect was attributed [53,54].

3.5. Di/Aryl alkanoids (*Curcuminoids, bisabolane-sesquiterpene derivatives)*

Aryl and diaryl alkanoids are characteristic polyphenols in *Curcuma,* particularly in *C. longa*. The curcuminoids are diaryl-heptanoids, classified as

bisabolane-type of sesquiterpenes. It imparts the distinguished yellow color and spice flavor of yellow curcuma and to which several therapeutic effects are attributed [3]. In this study, 23 di/aryl alkanoids were detected, predominantly in *C. longa* rhizome as shown in peaks 35-57 through Rt range 9.5-14.9 min, and were indeed previously reported in yellow curcuma [2,3,6,42,50]. In contrast, only 9 curcuminoids were detected in *C. caesia* as in peaks 35, 40, 45, 46, 47, 52, 53 and 54 (**Table 2**), and suggestive for activation of cucruminoids biosynthesis in *C. longa* as official drug in that taxa. Other diaryl alkanoids included furanone and pentadienone derivatives as in peaks 39, 41-43, 48 and 52 (**Table 2**).

Identification was based on reported fragmentation pathways and diagnostic product ions as explained in detail by Rasheed, et al., and Quirós-Fallas, et al.,[3,50] (**Suppl. Fig. S9**). For example, C_3- and C_5- di-keto curcuminoids such as curcumin I, II, III and their analogues, undergo heptanoid chain cleavage at C_4, followed by decarbonylation (-CO, 28 amu), demethylation and dehydroxylation (-CH_3-OH, 32 amu) to yield diagnostic ions, depending on aryl substitution, commonly detected at *m/z* 177, *m/z* 147, *m/z* 145, *m/z* 119 [3,50]. In case of a single C_3-keto alkanoids as in peaks 49 and 52, diagnostic product ion at *m/z* 137 for the neutral loss of substituted aryl moiety was observed as a result of precursor ion rearrangement followed by chain cleavage at C_1-C_2 bond [3,50]. In mono- or di-hydroxylated heptanoids, dehydrated product ion was detected (-H_2O, 18 amu). Whereas, cucruminoids having furanone ring in the central chain as curcumalongin A/B/C and others, as in peaks 39, 41-43 and 48 (**Table 2**), fragmentation pathway included cleavage of the 5-membered furanone ring preceded by precursor ion rearrangement to yield product ion at *m/z* 153 or *m/z* 123 [3]. Finally, the C_3-ester containing curcuminoids as in calebin A, peak 37 (**Table 2**) had cleavage at the ester linkage releasing diagnostic ions at *m/z* 177 and *m/z* 207 [3]. The mono-aryl heptanoids were detected exclusively in yellow curcuma at $[M+H]^+$ 217.1579; $C_{15}H_{21}O^+$ and 219.174; $C_{15}H_{23}O^+$ in peaks 56 and 57, and were

identified as turmerone and dihydroturmerone having diagnostic ions at *m/z* 119 and *m/z* 121, respectively,[50] (**Table 2**).

3.6. Sesquiterpenes

Sesquiterpenes are the major phytochemicals detected in genus *Curcuma*, where 328 compounds belonging to various subclasses were reported among 28 species [2]. In this study, 24 sesquiterpenes were tentatively identified in blue curcuma; peaks 58-81, several of which are reported for the first time in *C. caesia.* In contrast, only 7 of them were detected in yellow curcuma, peaks 65, 66,75, 77-80 (**Table 2**). Herein, sesquiterpenes were 5 germacrane (peaks 72, 73, 77-79), 1 elemane (peak 81), 1 carabrane (peak 76) and 17 guainane (guainolide) skeletons (**Table 2**) aside from the bisabaolane-type that was discussed in the previous subsection 3.2.5 [2,9,55]. *C. longa* had 2 types only i.e., 3 germacrane and 4 guainane. In contrast, *C. caesia* possessed the 4 subtypes of sesquiterpenes consistent with previously reported literature (**Fig. 3**) [2,9,55,56].

MS/MS Spectra distinguished between sesquiterpenes *via* observing product ions and their respective elemental formulae, that correspond to dehydration, decarboxylation, dealkylation and, most importantly, RDA fragmentation that allowed to discriminate between the different subtypes. For example, peaks 72, 75 and 76 had the same molecular ion and formula at $[M+H]^+$ 235.1685, $C_{15}H_{23}O_2^+$; the first, peak 72, showed fragments for the loss of water, carbonyl and isopropenyl side chain at *m/z* 217; $C_{15}H_{21}O^+$ (-H_2O, 18 amu), *m/z* 207; $C_{14}H_{23}O^+$ (-CO, 28 amu), *m/z* 189; $C_{14}H_{21}^+$ (-H_2O and -CO), *m/z* 193; $C_{12}H_{17}O_2^+$ (- isopropenyl $C_3H_6^+$) and *m/z* 147; $C_{11}H_{15}^+$ (loss of H_2O, CO and isopropenyl) followed by sequential delalkylation at *m/z* 135, *m/z* 121, *m/z* 107, *m/z* 93 and *m/z* 79 which is consistent with germacrone epoxide (germacrane type) (**Suppl. Fig. S10A**). The second, peak 75, showed dehydrated ion at *m/z* 217; $C_{15}H_{21}O^+$, pentyl-ring cleavage at *m/z* 179; $C_{11}H_{15}O_2^+$, and *m/z* 55; $C_4H_7^+$, RDA fragmentation of heptyl-ring at *m/z* 113; $C_6H_9O^+_2$, *m/z* 97; $C_6H_9O^+$ and *m/z* 69; $C_5H_9^+$, which is consistent with the

guainane-type sesquiterpene curcumenol (**Suppl. Fig. S10B**). Whereas, the carabrane-type curcumenone in peak 76 showed product ions for decarbonylation at *m/z* 207; $C_{14}H_{23}O^+$ (-CO, 28 amu), butanone-side chain cleavage at *m/z* 165; $C_{11}H_{17}O^+$ and *m/z* 71; $C_4H_7O^+$, propyl-ring cleavage and loss of butanone-side chain at *m/z* 151, $C_{10}H_{15}O^+$ and *m/z* 85, loss of isopropenyl and butanone side chain at *m/z* 123; $C_8H_{11}O^+$ (**Suppl. Fig. S10C**). In peak 81, epi/curzerenone is an elemane sesquiterpene that was previously reported in *C. caesia* [9]. The precursor ion was detected at $[M+H]^+$ 231.1374; $C_{15}H_{19}O_2^+$, which upon fragmentation resulted in diagnostic product ions at *m/z* 123; $C_7H_7O_2^+$ and *m/z* 109; $C_8H_{13}^+$ for the hexyl-ring cleavage, *m/z* 173; $C_{12}H_{13}O^+$ and *m/z* 55; $C_3H_3O^+$ for furanone ring cleavage, *m/z* 161 $C_{10}H_9O_2^+$ for the loss of isopropenyl and ethenyl substituents followed by further dealkylation at *m/z* 149 and *m/z* 137. Furthermore, product ion corresponding to the furanone ring was detected at *m/z* 83; $C_5H_7O^+$, and the hexanone ring moiety at *m/z* 95; $C_6H_7O^+$.

Zedoalactones and zedoarolides are guaianolides that were previously reported in *Curcuma*, including *C. longa* [50]. Whereas, the dihydro-derivative of zedoarolide B, peak 69, detected in *C. caesia* is, according to our knowledge, a newly detected metabolite (**Table 2**). The precursor ion was detected in negative ionization mode at $[M-H]^-$ 283.1543; $C_{15}H_{23}O_5^-$, having extra 2-hydogen atoms than zedoarolide B, peak 66, that was previously reported in *C. phaeocaulis and C. zedoaria* [2,6,55]. Fragmentation yielded product ions corresponding to decarboxylation ($-CO_2$, 44 amu) and 3 successive dehydration (-3X 18 amu) at *m/z* 265; $C_{15}H_{21}O_4^-$, *m/z* 239; $C_{14}H_{23}O_3^-$, *m/z* 221; $C_{14}H_{21}O_2^-$, *m/z* 203; $C_{14}H_{19}O^-$ and *m/z* 185; $C_{14}H_{17}^-$ (**Suppl. Fig.S11**). Other fragments included lactone ring cleavage at *m/z* 193, $C_{12}H_{17}O_2^-$, followed by sequential dealkylation and dehydration at *m/z* 169, $C_{10}H_{17}O_2^-$, *m/z* 151; $C_{10}H_{15}O^-$ and *m/z* 133, $C_{10}H_{13}^-$.

The myriad chemical reservoir of sesquiterpenes in *C. caesia* is a special feature that definitely has an impact on its therapeutic effects, particularly,

anticancer, anti-inflammatory, antimicrobial and hepatoprotective bioactivities among several others that are reported on each of its subclasses *via* different mechanisms of action [55]. Further studies are recommended to compare the bioactivity of the crude extract containing mixture of sesquiterpenes with that of the isolated components or subfractions, as well as conducting chronic and acute toxicity studies to determine its recommended daily intake dose.

3.3.7. Fatty acids (FA)/Glycerolipids (GL)

Fatty constituents were one of the major classes detected herein represented by 21 metabolites in negative ionization mode as in peaks 82-103 and were eluted at wide Rt range 6.6-17.2 min according to their relative polarity i.e. short-chain dicarboxylated/oxygenated FA were eluted earlier in contrast to long-chain FA glycerates (**Table 2**). Several metabolites were derivatives of palmitic, linoleic and oleic acids as evidenced by product ions at *m/z* 255; $C_{16}H_{31}O_2^-$, *m/z* 279; $C_{18}H_{31}O_2^-$ and *m/z* 281; $C_{18}H_{33}O_2^-$, respectively. Fragmentation included dehydration (-H_2O, 18 amu), decarboxylation (-COO, 44 amu) in addition to deglycosilation in case of glycated FA as in peak 91 detected in blue curcuma (**Table 2**). In phosphethanolamine derivatives, diagnostic ion at *m/z* 196 was detected as in peaks 92 and 93 (**Table 2**). Hydroxylated-oxo-penta/hexa-decanoic acids were detected in both species in peaks 88-90, in which hydroxy-oxohexadecanoic acid, peak 90, was previously reported in yellow curcuma [50].

3.4. Primary Metabolites Profiling of *C. longa* and *C. caesie via* GC-MS (Post-Silylation)

To assess variation of primary metabolites among *C. longa* and *C. caesie* to account for nutritive value and not readily ionized using ESI in UPLC-MS, GC–MS analysis was employed post-silylation (**Suppl. Fig. S12**). A total of 38 peaks were identified (**Table 3**) categorized into alcohols (2), fatty acids/esters (8), organic acids (5), sugars (7), alongside cinnamates (3), steroids/terpenes (13) as secondary metabolites. *C. longa* exhibited higher sugar level (40.5%),

followed by fatty acids/esters (27.4%). In contrast, *C. caesia* was dominated by steroids/terpenes (42.5%), with sugars (29.9%) as the second major component (**Fig. 4**), and to rationalize why *C. longa* is more suited for culinary uses than *C. caesia*. Differences among each class is explained below in more details in the next subsections.

3.4.1. Sugars

Sugars amounted as the main primary metabolite class in *C. longa* and *C. caesie* represented by a total of 7 peaks belonging to mono- and di-sugars. The relative higher sugar level in *C. longa* at 40.5% versus 29.93% in *C. caesia* infers for the improved taste and nutritive value *in C. longa*. Among sugars, sucrose was the most abundant sugar detected at 20.02% and 11.16% in *C. longa* and *C. caesia*, respectively. The presence of sucrose at substantial levels suggest for its role as sweat attribute in both species [29,57]. Following sucrose, talose was another major sugar detected at 10-12%, less common in dietary sources, though of potential health benefits. Compared with di-sugars that showed differences among species, mono-sugar represented by glucose was present at comparable levels *ca*. 5-6%. These results fall in accordance with previous proximate analysis of *C. caesia* and *C. longa* revealing substantial sugar content (19–21%) of dry weight [58], comparable to levels detected using GC/MS and extend here in to reveal for sucrose as the major form

3.4.2. Organic acids and alcohols

Organic acids were detected in both species at 8.2% and 5.6% in in *C. longa* and *C. caesia,* respectively (**Table 3**). Organic acids contribute to food attributes as natural preservative, food digestion, and in protein utilization [59], in addition to taste perception as a flavor enhancer. Major forms included 2-methyl-2-butenedioic acid dimethyl ester and glutaric acid, suggesting their potential use as food additive, preservation, and health-related effects. Compared to acids, alcohols, represented by glycerol and dodecanol, were

detected at much lower levels of 2.2-2.6% (**Table 3, Fig. 4**). Previous studies reported the presence of various alcohols including glycerol and monoterpene alcohols, in *Curcuma* essential oils [60].

3.4.3. Cinnamates

GC–MS analysis of *C. longa* and *C. caesia* extracts revealed much higher levels of cinnamates detected in C*. longa* than *C. caesia* at 4.5% and 0.3%, respectively. Examples of cinnamates included hydrocinnamic acid, 4-coumaric acid, and isoferulic/ferulic acid, with isoferulic/ferulic acid as major form in *C. longa* at 4.2%. The higher cinnamate level in *C. longa* suggests for stronger antioxidant and anti-inflammatory properties, as cinnamates are known for their role in human health [61,62].

3.4.4. Steroids/Terpenes

Steroids/terpenes were represented in *C. long* and *C. caesia* by 13 peaks, detected at much higher levels in *C. caesia* at 42.5% versus 17.1% in *C. longa*. Most notably, epicurzerenone was detected in *C. caesia* at 22.39% relative to *C. longa* at trace levels 0.09%. Epicurzerenone, a sesquiterpene, has been reported to exert potential antitumor and anti-inflammatory effects [63]. A study on essential oil analysis of *C. caesia* rhizomes reported less epicurzerenone (12.47%) comparable to levels detected here in this study [64]. Following epicurzerenone, 4,5-epoxygermacrone (12.14%) was the predominant sesquiterpene in *C. caesia*, suggesting a rich terpenoid profile associated with strong anti-inflammatory and antimicrobial activities [65]. Compared to *C. caesia, C. longa* is characterized by higher levels of αR-turmerone (7.13%) and curlone (3.59%), suggestive of differential terpenoids biosynthesis

Other sesquiterpenes detected at much lower levels included 4,5-epoxygermacrone (12.1%), valerenic acid (2%), zederone (1.9%), and curzerene (1.6%) in *C. caesia*, as well as curlone (3.6%), germacrone (3.6%), and curcumenone (1.3%) in *C. longa*.

3.4.5. Fatty acids/ esters

Fatty acids and esters represented the second and third most abundant metabolite class in *C. longa* and in *C. caesia*, respectively (**Table 3**). The higher fatty acid level in *C. longa* at 27.5% versus 19% in *C. caesia* highlights for improved nutritive value *in C. longa*, and is concurrent with the higher sugar profile. Among fatty acids/esters, palmitic acid was the major form detected at 14.2% and 10.2% in *C. longa* and *C. caesia*, respectively. The presence of palmitic acid at considerable levels in both *C. longa* and *C. caesia* suggests its role in energy metabolism [66]. A study on fatty acids composition of *C. longa* oil reported oleic acid likewise as the major component (56-58%) [67], slightly higher than that detected herein in alcohol extract using GC/MS .Following palmitic acid, stearic acid was the other major fatty acid at 4-6 %. Linoleic and oleic unsaturated fatty acids were detected at much lower levels in both species at 0.8-1.1 %, and suggestive that saturated fatty acids predominate in *Curcuma* species. . Asides from free fatty acids, acyl esters were likewise detected such as 1-monopalmitin, 1-monolinolein, and glycerol monostearate in both species at 0.1-2%.

3.5. Aroma Profiling of *C. longa* and *C. caesia* rhizomes *via* SPME coupled to GC-MS

SPME is well suited for the profiling of aroma and was employed for *C. longa* and *C. caesia* rhizomes, providing the real composition of their volatile blends, and is first time to be reported in both species via SPME-GC/MS (**Suppl. Fig. S13**). A total of 26 volatile constituents were detected in both *C. longa* and *C. caesia* rhizomes belonging to monoterpene hydrocarbon (6), oxide/ether (1), alcohol/aldehyde (2), sesquiterpene hydrocarbon (12), ketone (5), S-containing compounds (**Suppl.Table 2**). Both species showed comparable aroma composition, as seen in the relative percentile of each class in **Figure 5**. In *C. longa*, ketones, and sesquiterpenes were the major volatile classes, detected at 33.8% and 29.17%, respectively, whereas sesquiterpenes

were the most abundant in *C. caesia* (62.79%). Alcohol/aldehyde was detected in *C. longa* rhizomes at low levels (0.05%) versus monoterpenes detection at trace levels in *C. caesia* (1.18%). Tumerone was the major volatile in *C. longa* at 33.47 % followed by β-sesquiphellandrene at 20.82%, while β-elemene was the major form in C. caesia at 18.64% followed by heptanol and zingiberene at %15.1 and 12.8%, respectively. Interestingly, turmerone ketones were reported to be responsible for *C. longa* aroma [68], was detected at trace levels in *C. caesia* (0.01%). Turmerone was reported as a major constituent in the essential oil of *C. longa* at range 25.3-40.4 % [69], in accordance with our results using SPME. Likewise

3.6. Multivariate Data Analyses of blue curcuma *C. caesia* and yellow curcuma *C. longa* derived metabolome profiles

Classification models were attempted from the different analytical platforms i.e., UPLC/HR-MS/MS and GC-MS to identify discriminative metabolites for each species. Loading plots and S-plots identified biomarkers mediating for samples' classification as denoted by their Mol.wt./Rt derived from respective PCA and OPLS-DA plots

3.6.1. PCA and OPLS-DA analyses of UPLC/HR-MS/MS dataset

The unsupervised PCA model of UPLC/HR-MS/MS analyzed in negative ionization mode showed moderate prediction power (R2=0.7, Q2=0.55). Samples segregation was observed mostly along PC1 accounting for the major variance (**Fig. 6A**). PCA loading plot (**Fig. 6B**) revealed guainane-sesquiterpene "aerugidiol" as biomarker for *C. caesia* alongside other alkylbenzene sulfonate compounds at *m/z* 311 and *m/z* 325 (base peak *m/z* 183, $C_8H_7O_3S^-$). However, these are reported contaminants in irrigating waste water and pesticides used in agricultural field practice in China [70]. In contrast, *C. longa* was discriminated by exclusive presence of diarylheptanoids curcumin III and dihydrobisdemethoxycurcumin as well as abundance of curcumin I and

curcumin II which was further confirmed using supervised OPLS-DA score plot (R2=0.9, Q2=0.9) and respective S-loading plot (**Fig. 6C and 6D**).

On the other side, the PCA model derived from UPLC/HR-MS/MS data analyzed in positive ionization mode showed stronger classification as evidenced by larger variance and prediction power (R2=0.9, Q2=0.9), where PC1 and PC2 accounted for ca. 90% of the variance (**Fig. 6E**). *C. longa* specimen was still discriminated by diaryl heptanoids curcumin I, curcumin II, and curcumin III (**Fig. 6F)** and in agreement with negative mode result **(Fig. 6B)**, in addition to monoarylheptanoids ar-turmerone and dihydro-ar-turmerone revealed in positive mode, likely due to their improved ionization in that mode and highlighting the benefit of acquisition in both modes. In contrast, *C. caesia* was distinguished by guainane, germacrane, and elemane types of sesquiterpenes, namely curcumenol, germacrone epoxide, zederone, curdione, and epi/curzerenone. Supervised OPLS-DA was further employed for its superiority in biomarkers assignment (R2=0.9, Q2=0.9) **(Fig. 6G**). The S-loading plot of metabolites verified curcumin I, curcumin III, and dihydro-ar-turmerone as biomarkers of *C. longa,* while curdione and epi/curzerenone were the discriminatory metabolites of *C. caesia* (**Fig. 6H**). The results are consistent with previous studies reporting that *C. caesia* is among 4 *Curcuma* species only that biosynthesize mixture of 4 different types of sesquiterpenes (guainane, germacrene, elemane and carabrane), whereas diaryl heptanoids are detected in 10 *Curcuma* species including *C. longa* [9]. These results confirm that chemotaxonomic classification in *Curcuma* taxa is based on diarylheptanoids versus sesquiterpenes biosynthesis.

3.6.2. PCA and OPLS-DA analyses of GC/MS silylated metabolite dataset

PCA model of silylated compounds to encompass a total of 39 peaks analyzed *via* GC/MS showed good variance and prediction power (R2=0.9, Q2=0.8) where PC1 and PC2 accounted for > 70% of metabolites (**Fig. 7A**). Loading plot of metabolites assigned epicurzerenone sesquiterpene as biomarker for blue curcuma *C. caesia,* while yellow curcuma *C. longa* was

discriminated by abundance of palmitic acid, iso/ferulic acid, germacrone and arylheptanoid turmerone (**Fig. 7B**). These results are in agreement with UPLC/HR-MS/MS results shown in **Table 1 and Figures 6E-6H**. To verify classification, OPLS-DA was conducted, where S-plot assigned epicurzerenone as *C. caesia* discriminatory metabolite alongside epoxygermacrone. In contrast, sucrose was abundant in *C. longa* (**Fig. 7C and 7D**), and to account for the improved taste of *C. longa* and culinary use compared to *C. caesia*.

3.6.3. PCA and OPLS-DA analyses of SPME-GC/MS volatiles dataset

With regards to volatile components analyzed *via* SPME-GC/MS, PCA and OPLS-DA score plots showed likewise good variance and prediction power (R2=0.9, Q2=0.8-0.9) representing > 90% of the total variance (**Figure 7E).** Both loading and S-plots verified that turmerone and sesquiphellandrene are the discriminating volatiles of *C. longa* (**Fig. 7F and 7H**). PCA loading plot detected further enrichment of *C. caesia* aroma profile with alcohol i.e., heptanol, sesquiterpene hydrocarbons *β*-elemene, humulene, zingiberene and oxygenated ketone sesquiterpene epi/curzerenone (**Fig. 7F**). The S-plot verified further enrichment of *C. caesia* in heptanol and epi/curzerenone and considered its volatile biomarkers (**Fig. 7H**)**.** It's noteworthy that epi/curzerenone imparts a mushroom-like rooty odor of blue curcuma that is balanced with sweet and fresh herbal aroma attributed to sesquiterpenes hydrocarbons [71]. In contrast, turmerone essentially imparts the distinctive turmeric spicy odor in *C. longa* [72].

In conclusion, epi/curzerenone oxygenated sesquiterpene of elemane type were recognized as a discriminating metabolite for blue curcuma *C. caesia* based on UPLC/HR-MS/MS, post- silylated GC/MS, and SPME-GC/MS analyses. In contrast, *C. longa* is recognized with its mono-aryl and diaryl-heptanoids, in addition to its further enrichment in fatty acids, sugars, and cinnamates (**Fig. 6 & 7**)**.**

3.7. Quantification of total phenolic (TPC) and flavonoid contents (TFC) in *C. caesia* and *C. longa* rhizomes

The total phenolic and flavonoid contents were quantified in both turmeric samples for standardization purposes. The results revealed significant differences in both contents, where TPC in yellow curcuma (106.26±3.53 mg GAE/g w) was ~7 times higher than that in blue curcuma (16.64±0.14 mg GAE/g w) quantified as gallic acid equivalent. Similarly, TFC in yellow curcuma (18.45± 0.3 mg RE/g w) exhibited triple the flavonoid content of blue curcuma (6.43±0.27 mg RE/g w) quantified as rutin equivalent. The high TPC in yellow curcuma is compatible with its further enrichment with curcuminoids (Di/phenyl heptanoids) as revealed from UPLC/HR-MS/MS profiling and subsequent multivariate data analyses in contrast to blue curcuma (**Table 2, Fig 6**).

3.8. Bioactivity assays

3.8.1. Antioxidant activity determination:

Scavenging of free radicals is known to mediate for several bioactivities and serve as a good prediction for exploring the potentials of natural resources, thus both species were comparatively assayed for their free radical scavenging potential using 3 different *in vitro* assays viz. DPPH, ABTS and FRAP, measured as trolox equivalent. This ensured to have better validated evaluation of both turmeric extracts according to their lipophilic and hydrophilic constituents using different action mechanisms [73]. Yellow curcuma exhibited higher scavenging activity by DPPH (37.36 ± 0.99 mg TE/g w) and ABTS (34.37±0.74 mg TE/g w) assays than the blue curcuma (20.78±0.74 mg TE/g w and 18.31±0.18 mg TE/g w, respectively) which still showed moderate antioxidant activity. In contrast, FRAP assay which measures the reducing power or electron-donating capacity of compounds, revealed comparable antioxidant potential of blue (34.12±0.33 mg TE/g w) and yellow curcuma (31.44±0.93 mg TE/g w). The obtained results are compatible with the enriched phenolic content in yellow curcuma that are potent scavengers of free radicals, as well

as, the presence of hydroquinone derivatives detected *via* UPLC/HR-MS/MS in blue curcuma that are potent ferric reductants, thus reflected in the FRAP assay [45] (**Table 2**).

3.8.2. Antidiabetic activity determination via α-glucosidase inhibition

Both blue and yellow curcuma are reported to exhibit *in vivo* antidiabetic activity [74,75]. In this study their α-glucosidase inhibition activity was determined comparably against acarbose reference drug. *C. longa* showed more potent activity evidenced by lower IC_{50} (0.325±0.025 mg/ml) than that observed for *C. caesia* rhizome (1.04±0.064 mg/mL) and acarbose (0.4891 ±0.1 mg/mL). This is justified by the further abundance of phenolics in *C. longa* which interfere with the active sites of α-glucosidase, thus, preventing it from binding with carbohydrates [76]. Moreover, curcuminoids are proven by clinical and preclinical trials to act synergistically against diabetes *via* different mechanism of action [6,77]. On the other side, terpenes of *C. caesia* showed high *in silico* binding affinity to α-glucosidase enzyme that contributes in the herein observed antidiabetic activity [78].

3.8.3. Anti-obesity activity determination via lipase inhibition

Rhizome extracts of *C. longa* and *C. caesia* were investigated for their anti-obesity activity using orlistat reference drug *via* lipase inhibition. Both samples showed no significant inhibitory activity against lipase at the maximal test concentration (10 mg/mL) and its dilutions (orlistat IC_{50}=0.16±0.08 mg/mL).

4- Conclusion

The study presented the first integrated comparative metabolome profiling of *C. caesia* and *C. longa* using multiplex approach aided by multivariate data analyses, uncovering distinct metabolic divergence among both species and highlighting several first-time reported metabolites in the less explored turmeric blue curcuma. The analyses revealed for 11 metabolites annotated

via NMR, 110 tentatively identified metabolites by UPLC/HR-MS/MS, 38 silylated compounds and 26 volatiles detected by GC/MS analysis. Samples' classification and discriminatory chemotaxonomic biomarkers were assigned for each species by PCA and OPLS data analyses emphasizing diverse sesquiterpenes in *C. caesia vs* curcuminoids and sugar enrichment in *C. longa* aligning with its established culinary and therapeutic uses. Antioxidant and antidiabetic bioassays showed superior activity of *C. longa* compatible with its higher quantified contents of total phenolics and flavonoids, whereas both species were inactive as anti-obesity agents compared to orlistat reference drug. Targeted isolation of novel sesquiterpenes annotated in *C. caesia* is recommended for therapeutic evaluation to elucidate its potential in pharmaceutical and food industries.

Acknowledgement

Authors would like to thank Dr. Kai Wang at the Chinese Academy of Sciences, Beijing for sample collection and authentication

Conflict of interests

Authors declare that there is no conflict of interests

Funding

Authors declare no funding was received

Dataset availability

The raw files dataset used and/or analyzed during the current study available from the corresponding author on reasonable request.

References

1 Rahaman, M. M. *et al.* The Genus Curcuma and Inflammation: Overview of the Pharmacological Perspectives. *Plants (Basel, Switzerland)* **10**, doi:10.3390/plants10010063 (2020).

2 Sun, W. *et al.* Chemical constituents and biological research on plants in the genus Curcuma. *Critical reviews in food science and nutrition* **57**, 1451-1523 (2017).

3 Quirós-Fallas, M. I. *et al.* Polyphenolic HRMS Characterization, Contents and Antioxidant Activity of Curcuma longa Rhizomes from Costa Rica. *Antioxidants* **11**, 620 (2022).

4 Ye, Y. *et al.* The use of widely targeted metabolomics profiling to quantify differences in medicinally important compounds from five Curcuma (Zingiberaceae) species. *Industrial Crops and Products* **175**, 114289, doi:https://doi.org/10.1016/j.indcrop.2021.114289 (2022).

5 Borah, A., Kumar, D., Paw, M., Begum, T. & Lal, M. A review on ethnobotany and promising pharmacological aspects of an endangered medicinal plant, Curcuma caesia Roxb. *Turkish Journal of Botany* **44**, 205-213 (2020).

6 Elhawary, E. A., Moussa, A. Y. & Singab, A. N. B. Genus Curcuma: chemical and ethnopharmacological role in aging process. *BMC Complementary Medicine and Therapies* **24**, 31, doi:10.1186/s12906-023-04317-w (2024).

7 Dutta, B. Study of secondary metabolite constituents and curcumin contents of six different species of genus Curcuma. *J. Med. Plants Stud* **3**, 116-119 (2015).

8 Ibrahim, N. N. A. *et al.* A Comprehensive Review with Future Prospects on the Medicinal Properties and Biological Activities of Curcuma caesia Roxb. *Evidence-Based Complementary and Alternative Medicine* **2023**, 7006565, doi:https://doi.org/10.1155/2023/7006565 (2023).

9 Vairappan, C. S., Elias, U. M., Ramachandram, T. R. & Kamada, T. Secondary metabolites from rhizome of Curcuma caesia Roxb.(Zingiberaceae). *Biochem. Syst. Ecol* **48**, 107-110 (2013).

10 El-Hawary, E. A. *et al.* How Does LC/MS Compare to UV in Coffee Authentication and Determination of Antioxidant Effects? Brazilian and Middle Eastern Coffee as Case Studies. *Antioxidants* **11**, 131 (2022).

11 Farrag, A. F. S. *et al.* Unveiling metabolome heterogeneity in seed and husk from three cardamom species for quality control and valorization purposes of its waste products via NMR-based metabolomics in relation to in vitro biological effects. *Food chemistry* **480**, 143687, doi:10.1016/j.foodchem.2025.143687 (2025).

12 Netrprachit, P. *et al.* Bioactive compounds of pigmented rice extracts reveal by NMR-based metabolomics. *CyTA-Journal of Food* **21**, 760-770 (2023).

13 Farag, M. A., Porzel, A. & Wessjohann, L. A. Comparative metabolite profiling and fingerprinting of medicinal licorice roots using a multiplex

approach of GC–MS, LC–MS and 1D NMR techniques. *Phytochemistry* **76**, 60-72, doi:https://doi.org/10.1016/j.phytochem.2011.12.010 (2012).

14 El-Akad, R. H., El-Din, M. G. S. & Farag, M. A. How does Lagenaria siceraria (Bottle Gourd) metabolome compare to Cucumis sativus (Cucumber) F. Cucurbitaceae? A multiplex approach of HR-UPLC/MS/MS and GC/MS using molecular networking and chemometrics. *Foods* **12**, 771 (2023).

15 Ismail, W. M., Zayed, A., Ramadan, N. S., Sakna, S. T. & Farag, M. A. GC-MS based nutritional and aroma profiling of date palm seeds collected from different Egyptian cultivars for valorization purposes. *Scientific Reports* **15**, 16531 (2025).

16 Babotă, M. *et al.* Phytochemical analysis, antioxidant and antimicrobial activities of Helichrysum arenarium (L.) Moench. and Antennaria dioica (L.) Gaertn. flowers. *Molecules (Basel, Switzerland)* **23**, 409 (2018).

17 Dezsi, Ș. *et al.* Antimicrobial and antioxidant activities and phenolic profile of Eucalyptus globulus Labill. and Corymbia ficifolia (F. Muell.) KD Hill & LAS Johnson leaves. *Molecules (Basel, Switzerland)* **20**, 4720-4734 (2015).

18 Zayed, A. *et al.* Olive solid wastes: UHPLC-MS/MS-based biochemometric approach for investigating the effect of conventional versus modern extraction methods on in vitro antioxidant, α-glucosidase, and lipase actions. *Food Bioscience* **62**, 105496, doi:https://doi.org/10.1016/j.fbio.2024.105496 (2024).

19 Nicolescu, A. *et al.* Potential therapeutic applications of infusions and hydroalcoholic extracts of Romanian glutinous sage (Salvia glutinosa L.). *Frontiers in Pharmacology* **13**, 975800 (2022).

20 Tanase, C. *et al.* Biological and chemical insights of beech (Fagus sylvatica L.) bark: A source of bioactive compounds with functional properties. *Antioxidants* **8**, 417 (2019).

21 Sanneur, K. *et al.* Inhibitory Effects of Saponin-Rich Extracts from Pouteria Cambodiana against Digestive Enzymes α-Glucosidase and Pancreatic Lipase. *Foods* **12**, 3738 (2023).

22 Matěnová, M. *et al.* Energy transfer in aggregates of bacteriochlorophyll c self-assembled with azulene derivatives. *Physical Chemistry Chemical Physics* **16**, 16755-16764 (2014).

23 Zheng, J.-J. *et al.* Ochracenoids A and B, Guaiazulene-Based Analogues from Gorgonian Anthogorgia ochracea Collected from the South China Sea. *Marine Drugs* **12**, 1569-1579 (2014).

24 Akram, W. *et al.* Guaiazulene and related compounds: A review of current perspective on biomedical applications. *Life Sciences* **316**, 121389, doi:https://doi.org/10.1016/j.lfs.2023.121389 (2023).

25 Tsuchiya, T. *et al.* Intense absorption of azulene realized by molecular orbital inversion. *Chemical Communications* **59**, 10604-10607, doi:10.1039/D3CC02311G (2023).

26 Migalska-Zalas, A., El kouari, Y. & Touhtouh, S. Methodologies for computing UV–VIS spectra and nonlinear properties of azo-azulene

derivatives. *Optical Materials* **34**, 1639-1643, doi:https://doi.org/10.1016/j.optmat.2012.03.021 (2012).

27 Bustamam, M. S. A. *et al.* Discriminating Metabolites of Curcuma caesia and Kaempferia parviflora through 1H-NMR and GC-MS Analysis for Plant Authentication. *Records of Natural Products* **19**, 74 (2025).

28 Mahanta, B. P. *et al.* A 1H-NMR spectroscopic method for the analysis of thermolabile chemical markers from the essential oil of black turmeric (Curcuma caesia) rhizome: application in post-harvest analysis. *Phytochemical Analysis* **31**, 28-36 (2020).

29 Jung, Y. *et al.* Metabolite profiling of Curcuma species grown in different regions using 1 H NMR spectroscopy and multivariate analysis. *Analyst* **137**, 5597-5606 (2012).

30 Wang, H., Su, G., Chen, G., Bai, J. & Pei, Y. 1H NMR-based metabonomics of the protective effect of Curcuma longa and curcumin on cinnabar-induced hepatotoxicity and nephrotoxicity in rats. *Journal of Functional Foods* **17**, 459-467 (2015).

31 Ain Ibrahim, N. N. *et al.* 1H NMR-based metabolomics approach revealing metabolite variation of black turmeric (Curcuma caesia) extracts and correlation with its antioxidant and α-glucosidase inhibitory activities. *Food technology and biotechnology* **61**, 104-117 (2023).

32 Oon, S. F. *et al.* Hypolipidemic activities of xanthorrhizol purified from centrifugal TLC. *Biochemical and Biophysical Research Communications* **478**, 1403-1408 (2016).

33 Flores-Frias, E. *et al.* Use of Curcuma and curcumin as a green corrosion inhibitors for carbon steel in sulfuric acid. *International Journal of Electrochemical Science* **14**, 5026-5041 (2019).

34 Khattab, A. R. *et al.* Assessing phytoequivalency of four Zingiberaceae spices (galangals, turmeric and ginger) using a biochemometric approach: A case study. *Industrial Crops and Products* **188**, 115722 (2022).

35 Pintatum, A. *et al.* In vitro anti-inflammatory, anti-oxidant, and cytotoxic activities of four Curcuma species and the isolation of compounds from Curcuma aromatica rhizome. *Biomolecules* **10**, 799 (2020).

36 Fuloria, S. *et al.* A comprehensive review on the therapeutic potential of Curcuma longa Linn. in relation to its major active constituent curcumin. *Frontiers in Pharmacology* **13**, 820806 (2022).

37 Jakubczyk, K., Drużga, A., Katarzyna, J. & Skonieczna-Żydecka, K. Antioxidant potential of curcumin—A meta-analysis of randomized clinical trials. *Antioxidants* **9**, 1092 (2020).

38 Paudel, A., Khanal, N., Khanal, A., Rai, S. & Adhikari, R. Pharmacological insights into Curcuma caesia Roxb., the black turmeric: a review of bioactive compounds and medicinal applications. *Discover Plants* **1**, 1-19 (2024).

39 Elghonemy, M. M. *et al.* Anticryptosporidial action mechanisms of Launaea spinosa extracts in Cryptosporidium parvum experimentally infected mice in relation to its UHPLC-MS metabolite profile and

biochemometric tools. *PLOS ONE* **20**, e0317497, doi:10.1371/journal.pone.0317497 (2025).

40 Macias-Benitez, S. *et al.* Rhizospheric Organic Acids as Biostimulants: Monitoring Feedbacks on Soil Microorganisms and Biochemical Properties. *Frontiers in Plant Science* **Volume 11 - 2020**, doi:10.3389/fpls.2020.00633 (2020).

41 Lin, D. *et al.* An Overview of Plant Phenolic Compounds and Their Importance in Human Nutrition and Management of Type 2 Diabetes. *Molecules (Basel, Switzerland)* **21**, doi:10.3390/molecules21101374 (2016).

42 Segneanu, A.-E., Vlase, G., Lukinich-Gruia, A. T., Herea, D.-D. & Grozescu, I. Untargeted Metabolomic Approach of Curcuma longa to Neurodegenerative Phytocarrier System Based on Silver Nanoparticles. *Antioxidants* **11**, 2261 (2022).

43 Satoh, T., McKercher, S. R. & Lipton, S. A. Nrf2/ARE-mediated antioxidant actions of pro-electrophilic drugs. *Free Radical Biology and Medicine* **65**, 645-657 (2013).

44 Spenceri, E. A. Disorders of pigmentation. *Facial Plastic Surgery Clinics of North America* **11**, 209-217, doi:https://doi.org/10.1016/S1064-7406(02)00026-3 (2003).

45 Ems, T., St Lucia, K. & Huecker, M. R. Biochemistry, iron absorption. (2017).

46 Aguiar, A. & Ferraz, A. Effect of aqueous extracts from Ceriporiopsis subvermispora-biotreated wood on the decolorization of Azure B by Fenton-like reactions. *International Biodeterioration & Biodegradation* **74**, 61-66, doi:https://doi.org/10.1016/j.ibiod.2012.07.010 (2012).

47 Kantasrila, R. *et al.* Ethnobotany and phytochemistry of plants used to treat musculoskeletal disorders among Skaw Karen, Thailand. *Pharmaceutical biology* **62**, 62-104, doi:10.1080/13880209.2023.2292261 (2024).

48 Arruda, H. S., Angolini, C. F. F., Eberlin, M. N., Pastore, G. M. & Marostica Junior, M. R. UHPLC-ESI-QTOF-MS/MS Profiling of Phytochemicals from Araticum Fruit (Annona crassiflora Mart.) and Its Antioxidant Activity. *Foods* **12**, 3456 (2023).

49 Elbatreek, M. H., Mahdi, I., Ouchari, W., Mahmoud, M. F. & Sobeh, M. Current advances on the therapeutic potential of pinocembrin: An updated review. *Biomedicine & Pharmacotherapy* **157**, 114032, doi:https://doi.org/10.1016/j.biopha.2022.114032 (2023).

50 Rasheed, D. M., Farag, M. A., Khattab, A. R., Rahman, M. F. A. & El-Haddad, A. E. A comparative MS-based metabolomics study and in-vitro antidiabetic assay of galangals, turmeric and ginger aided by molecular networking and chemometrics. *Industrial Crops and Products* **205**, 117438 (2023).

51 Li, K. *et al.* Rapid identification of anthocyanin from the epicarp of kadsura coccinea (lem.) AC Smith by UHPLC-Q-exactive orbitrap mass spectrometry. *Food Analytical Methods* **14**, 2545-2555 (2021).

52 Allen F, Greiner R & D, W. Competitive fragmentation modeling of ESI-MS/MS spectra for putative metabolite identification. *Metabolomics* **11**, 98-110, doi:10.1007/s11306-014-0676-4 (2015).
53 Khaledi, M. *et al.* A Comprehensive Review of Herbal Recommendations with the Potential to Inhibit COVID-19 Infection. *Journal of Medical Bacteriology* (2023).
54 Tateishi, K., Shibata, H. & Matsushima, Y. Isolation of zeanoside C, a new metabolite of IAA from corn (Zea mays L.) kernels. *Agricultural and biological chemistry* **52**, 3231-3233 (1988).
55 Afzal, A., Oriqat, G., Akram Khan, M., Jose, J. & Afzal, M. Chemistry and biochemistry of terpenoids from Curcuma and related species. *Journal of Biologically Active Products from Nature* **3**, 1-55 (2013).
56 Al-Amin, M., Eltayeb, N. M., Khairuddean, M. & Salhimi, S. M. Bioactive chemical constituents from Curcuma caesia Roxb. rhizomes and inhibitory effect of curcuzederone on the migration of triple-negative breast cancer cell line MDA-MB-231. *Natural Product Research* **35**, 3166-3170 (2021).
57 Van Hung, P. & Vo, T. N. D. Structure, physicochemical characteristics, and functional properties of starches isolated from yellow (Curcuma longa) and black (Curcuma caesia) turmeric rhizomes. *Starch-Stärke* **69**, 1600285 (2017).
58 Das, R., Mahapatra, S., Das, M. & Nayak, R. Estimation of carbohydrate, protein, and secondary metabolites of selected Curcuma species from the Northern coastal region of Odisha, India. *Journal of Pharmacognosy and Phytochemistry* **12**, 25-29 (2023).
59 Farag, M. A., Goyal, V. & Baky, M. H. Comparative metabolome variation in Brassica juncea different organs from two varieties as analyzed using SPME and GCMS techniques coupled to chemometrics. *Scientific Reports* **14**, 19900 (2024).
60 Poudel, D. K. *et al.* Analysis of Volatile Constituents in Curcuma Species, viz. C. aeruginosa, C. zedoaria, and C. longa, from Nepal. *Plants* **11**, 1932 (2022).
61 Erdoğan, Ü. & Erbaş, S. Phytochemical profile and antioxidant activities of Zingiber officinale (ginger) and Curcuma longa L.(turmeric) rhizomes. *Bilge International Journal of Science and Technology Research* **5**, 1-6 (2021).
62 Gogoi, N. G. *et al.* Enhanced biological activity of Curcumin Cinnamates: an experimental and computational analysis. *Medicinal Chemistry Research* **31**, 2195-2208 (2022).
63 Anjum, A. & Quraishi, A. Enhanced epicurzerenone production via in vitro elicitation of microrhizomes of Curcuma caesia Roxb. *In Vitro Cellular & Developmental Biology-Plant* **59**, 825-838 (2023).
64 Khuntia, S., Sahoo, B. C., Lenka, J., Kar, B. & Sahoo, S. In-silico prediction and in vitro validation of antioxidant, antibacterial and antifungal potential of Black Turmeric (Curcuma caesia Roxb.) essential oils and its constituents. *Industrial Crops and Products* **203**, 117185 (2023).

65 Paw, M. *et al.* Study of anti-oxidant, anti-inflammatory, genotoxicity, and antimicrobial activities and analysis of different constituents found in rhizome essential oil of Curcuma caesia Roxb., collected from north east India. *Current pharmaceutical biotechnology* **21**, 403-413 (2020).

66 Farag, M. A., Ramadan, N. S., Shorbagi, M., Farag, N. & Gad, H. A. Profiling of primary metabolites and volatiles in apricot (Prunus armeniaca L.) seed kernels and fruits in the context of its different cultivars and soil type as analyzed using chemometric tools. *Foods* **11**, 1339 (2022).

67 Paul, B., Munshi, M., Ahmed, M., Saha, G. & Roy, S. The fatty acid composition and properties of oil extracted from fresh rhizomes of turmeric (Curcuma longa Linn.) cultivars of Bangladesh. *Bangladesh Journal of Scientific and Industrial Research* **46**, 127-132 (2011).

68 Hasegawa, T., Nakatani, K., Fujihara, T. & Yamada, H. J. N. P. C. Aroma of turmeric: Dependence on the combination of groups of several odor constituents. **10**, 1934578X1501000663 (2015).

69 Naz, S., Ilyas, S., Parveen, Z. & Javed, S. J. A. J. o. C. Chemical analysis of essential oils from turmeric (Curcuma longa) rhizome through GC-MS. **22**, 3153 (2010).

70 Wang, Z. *et al.* Effects of microcystin-LR, linear alkylbenzene sulfonate and their mixture on lettuce (Lactuca sativa L.) seeds and seedlings. *Ecotoxicology* **20**, 803-814, doi:10.1007/s10646-011-0632-2 (2011).

71 Mahanta, B. P., Lahon, D., Kalita, D., Lal, M. & Haldar, S. Study on aroma-profile, key odorants and ontogenetic variability of black turmeric (Curcuma caesia Roxb.) essential oil: An aroma perspective. *Industrial Crops and Products* **193**, 116115, doi:https://doi.org/10.1016/j.indcrop.2022.116115 (2023).

72 Hasegawa, T., Nakatani, K., Fujihara, T. & Yamada, H. Aroma of turmeric: Dependence on the combination of groups of several odor constituents. *Natural Product Communications* **10**, 1934578X1501000663 (2015).

73 Thaipong, K., Boonprakob, U., Crosby, K., Cisneros-Zevallos, L. & Byrne, D. H. Comparison of ABTS, DPPH, FRAP, and ORAC assays for estimating antioxidant activity from guava fruit extracts. *Journal of food composition and analysis* **19**, 669-675 (2006).

74 Ibrahim, N. N. A. *et al.* A Comprehensive Review with Future Prospects on the Medicinal Properties and Biological Activities of Curcuma caesia Roxb.. *Evidence-Based Complementary and Alternative Medicine* **2023**, 7006565, doi:10.1155/2023/7006565 (2023).

75 Silva, P., Arawwawala, L., Kumari, M. & Galappatthy, P. Effect of Curcuma longa L. and curcumin on diabetes and it's complications: A review. *Journal of Ayurvedic and Herbal Medicine* **7**, 109-118 (2021).

76 Ali, A., Cottrell, J. J. & Dunshea, F. R. Antioxidant, Alpha-Glucosidase Inhibition Activities, In Silico Molecular Docking and Pharmacokinetics Study of Phenolic Compounds from Native Australian Fruits and Spices.

Antioxidants (Basel, Switzerland) **12**, doi:10.3390/antiox12020254 (2023).

77 Pokhrel, A., Chong, K. T. & Tayara, H. Therapeutic potential of curcuminoids in type 2 diabetes mellitus (T2DM): Insights from network pharmacology, molecular docking, and dynamics simulations. *Food Bioscience* **68**, 106406, doi:https://doi.org/10.1016/j.fbio.2025.106406 (2025).

78 Rathi, J., Faujdar, S., Dhiman, A., Yadav, R. & Kumar, P. MOLECULAR DOCKING BASED ANTIDIABETIC SCREENING OF CURCUMA CAESIA ROXB.

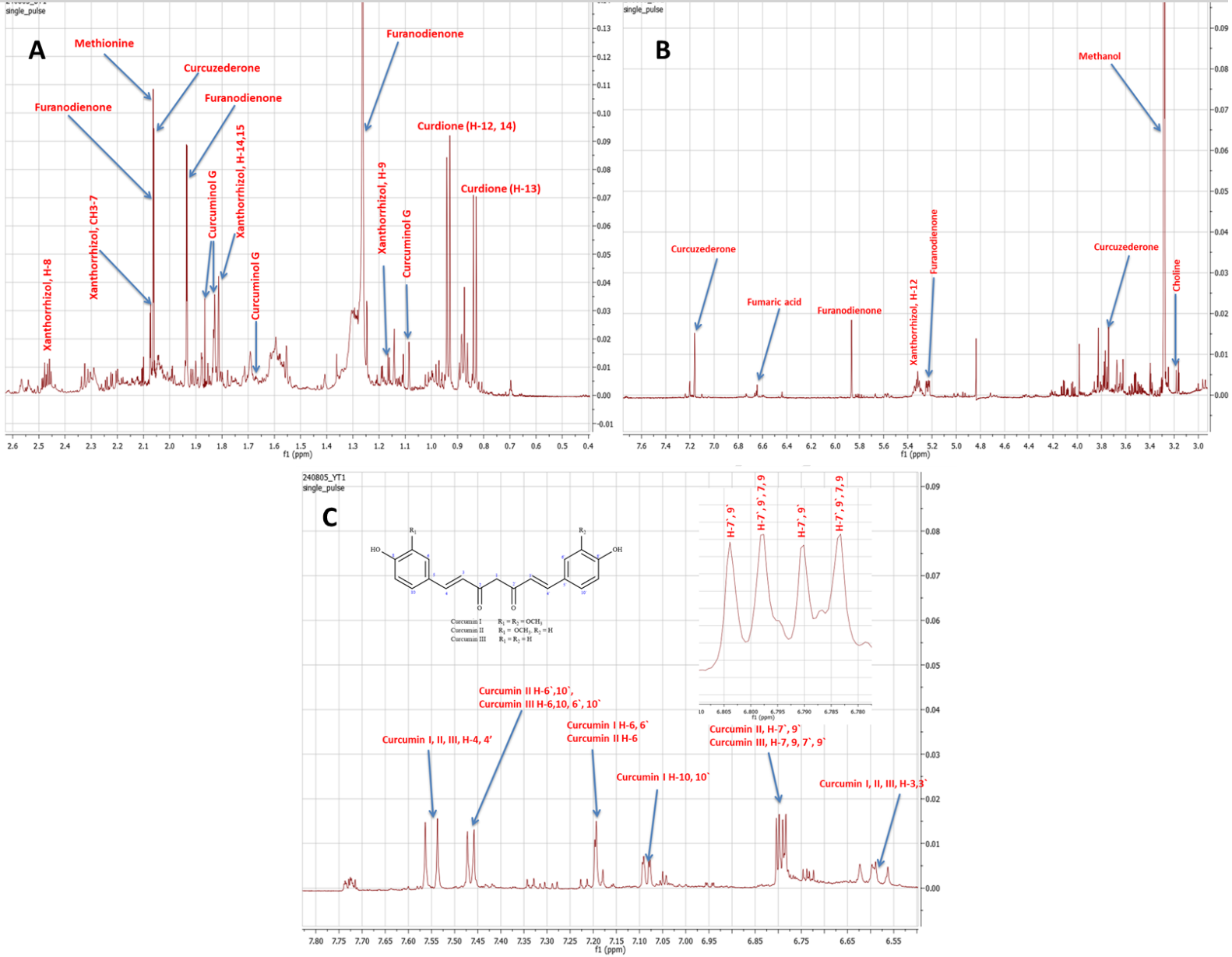

Figure 1: ^{1}H-NMR spectra (CD_3OD, 500 MHz) of *Curcuma caesia* (A,B: δ_H: 0–8 ppm) and *Curcuma longa* (C, δ_H: 6.5–8 ppm) used in the curent study. The spectra are labelled with maor key metabolites, while peaks assignments are summerized in Table 1

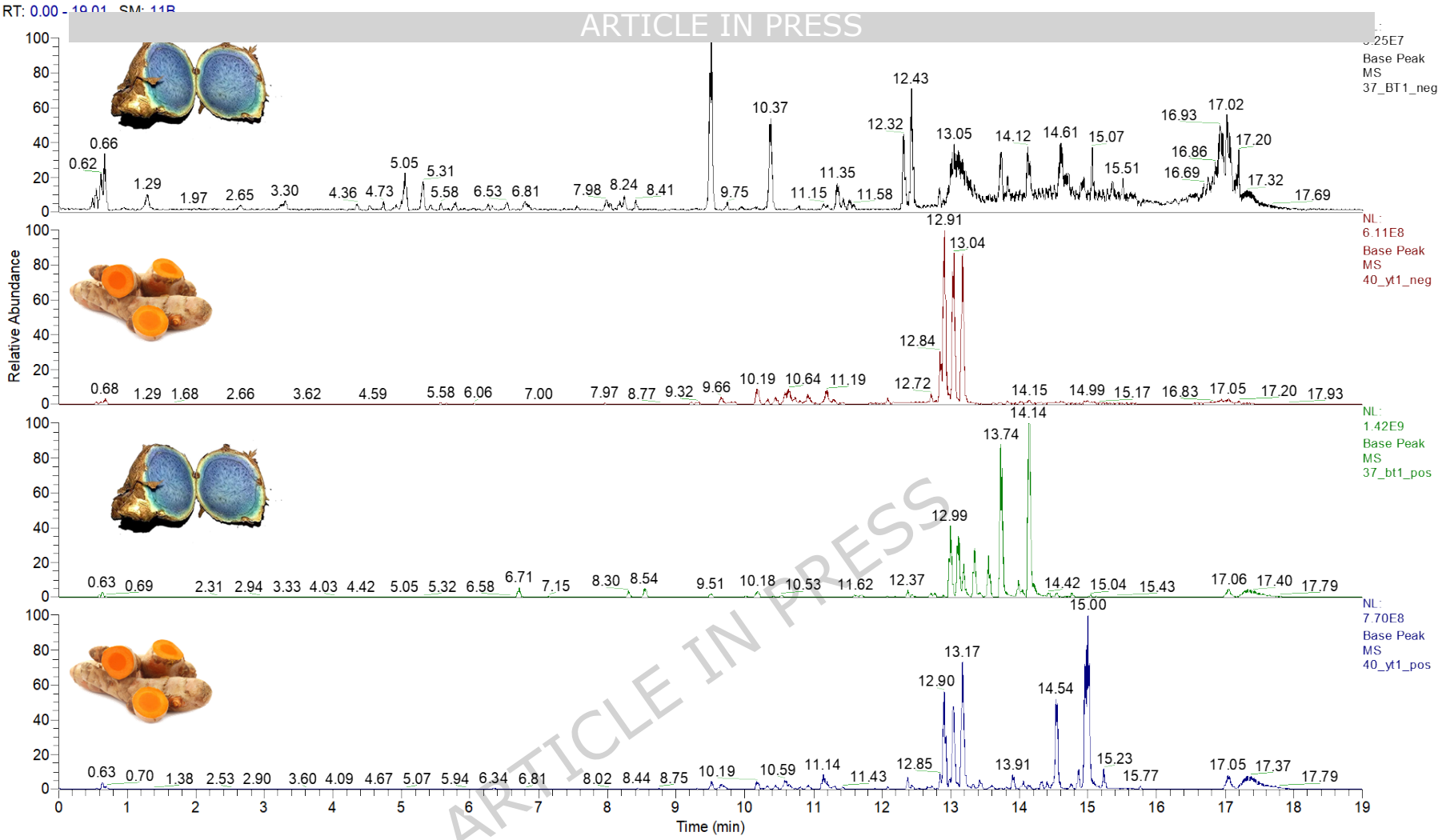

Figure 2: Base peak chromatograms of *C. Caesia* (blue curcuma) and *C. longa* (yellow curcuma) crude methanol extracts analyzed *via* UPLC/HR-MS/MS in both negative and positive modes

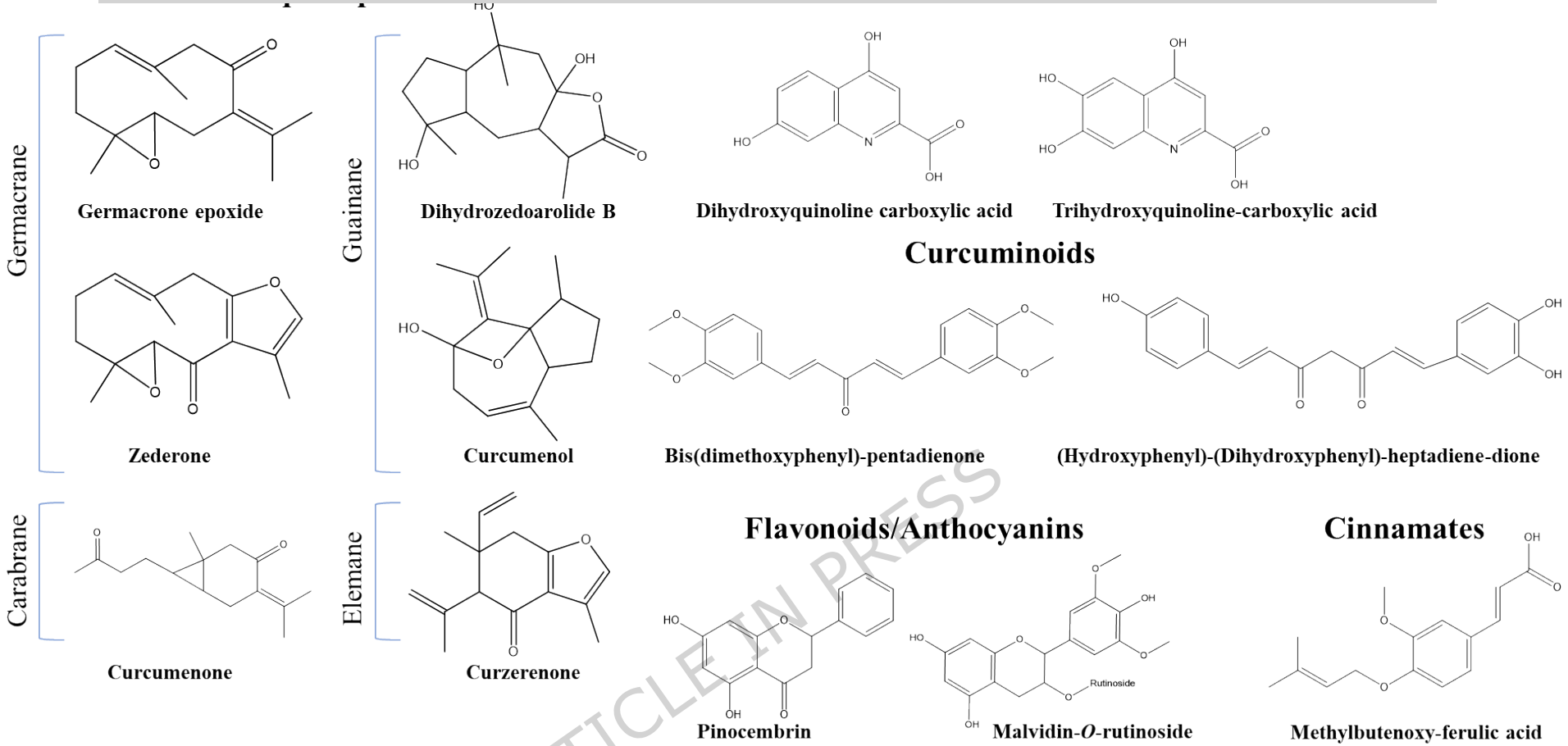

Figure 3: Structures of selected metabolites tentatively identified *via* UPLC/HR-MS/MS analysis in *C. caesia* and *C. longa* extracts as shown in Table 1

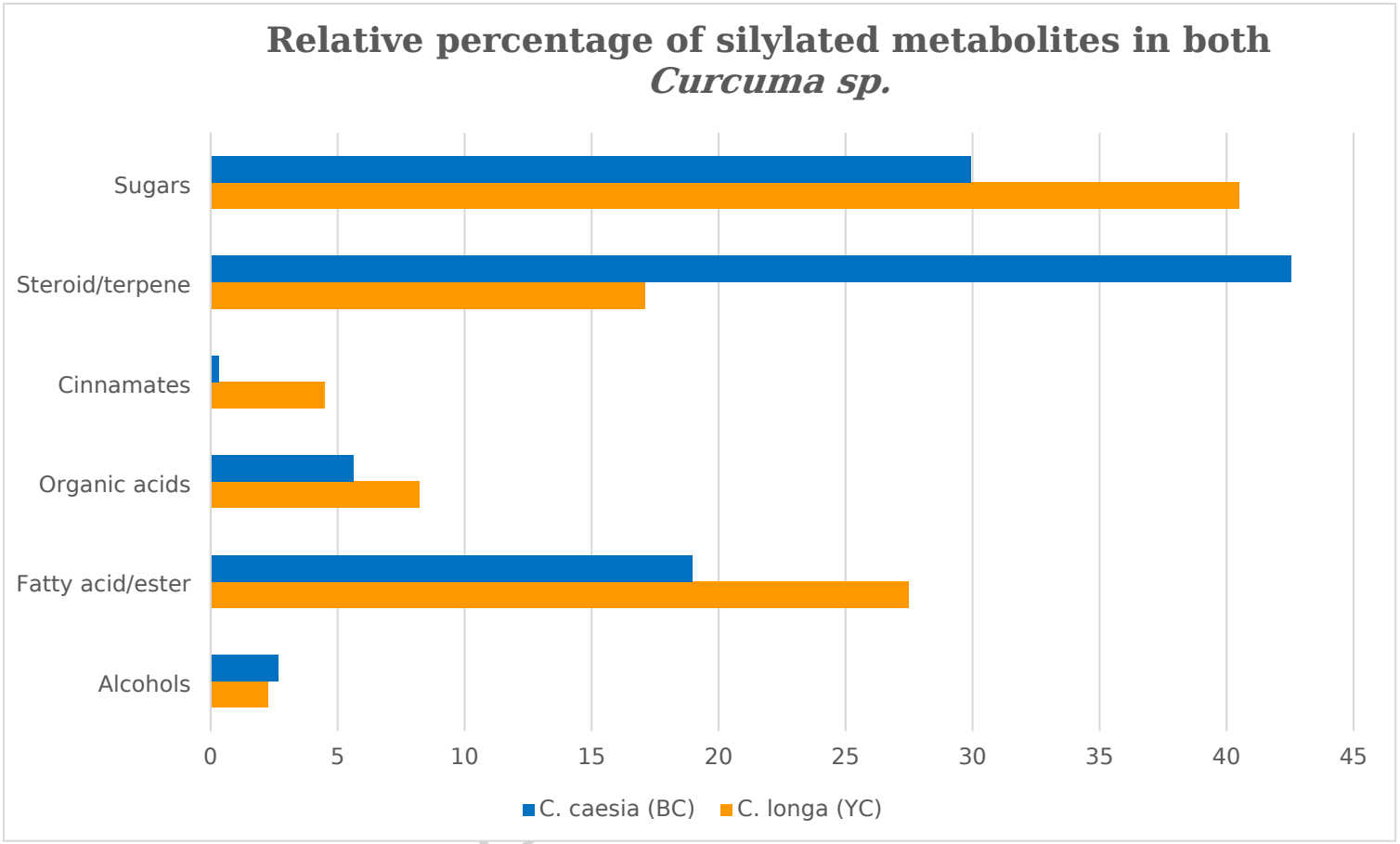

Figure 4: Relative percentage of silylated metabolites detected in *C. caesia* (blue) and *C. longa* (yellow) rhizomes *via* GC/MS analysis

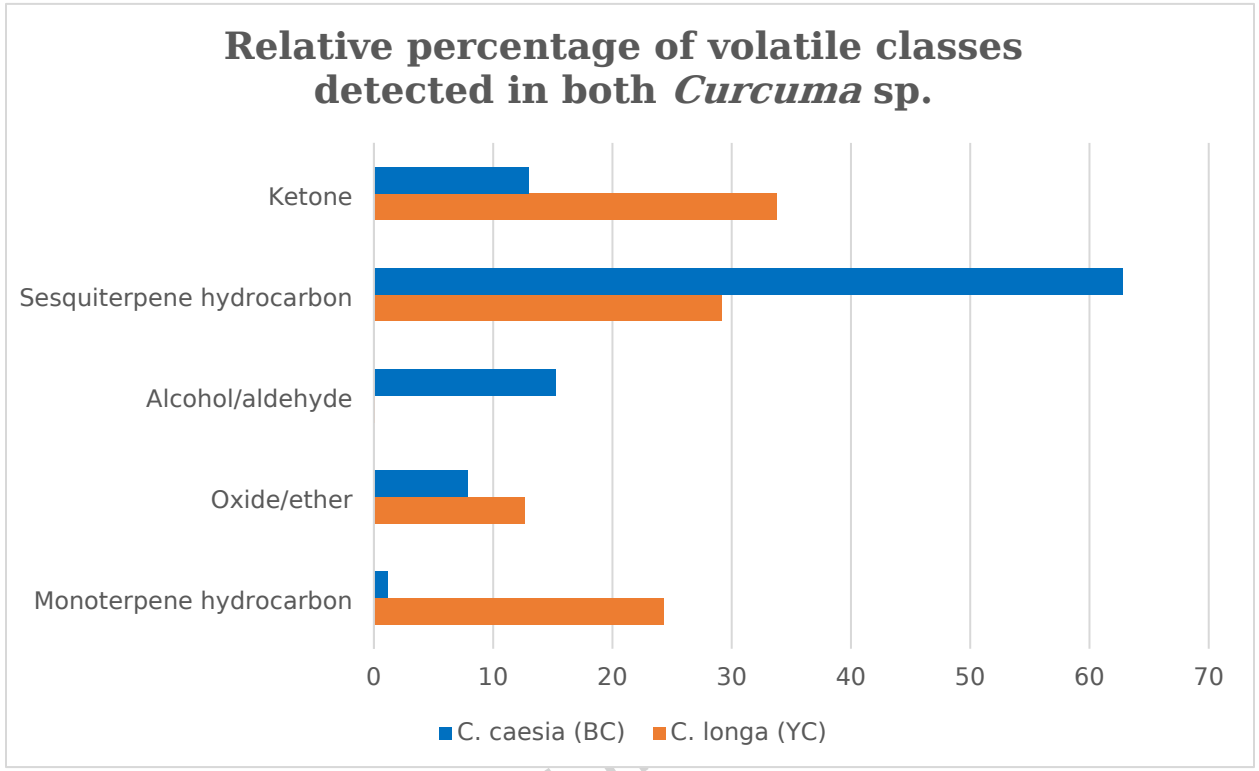

Figure 5: Relative percentage of aroma compounds detected in *C. caesia* (blue) and *C. longa* (yellow) *via* SPME-GC/MS analysis

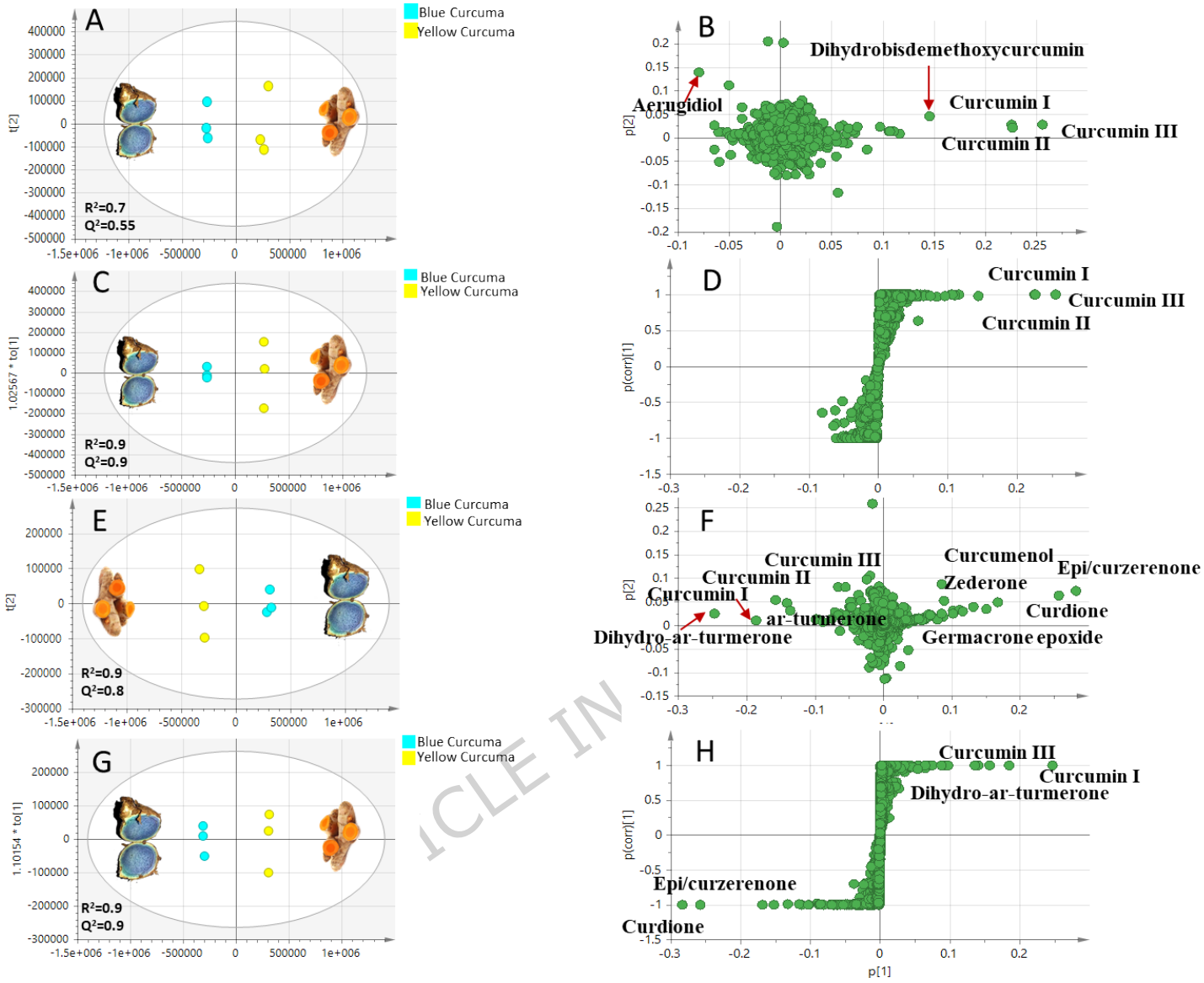

Figure 6: Multivariate data analyses of UPLC/HR-MS/MS dataset of blue curcuma (*C. caesia*) and yellow curcuma (*C. longa*) in both negative (A-D) and positive (E-H) ionization modes (n=3). Principle component analysis (PCA) score plots (A, E) and loading plots (B, F); orthogonal partial least squares discriminant analysis (OPLS-DA) score plots (C, G) and S-loading plots (D, H) with PC1 and PC2 represent >60% and > 90% of total variation in data derived from negative and positive ionization modes, respectively. Metabolites were assigned based on Mol.wt/Rt as identified in Table 1.

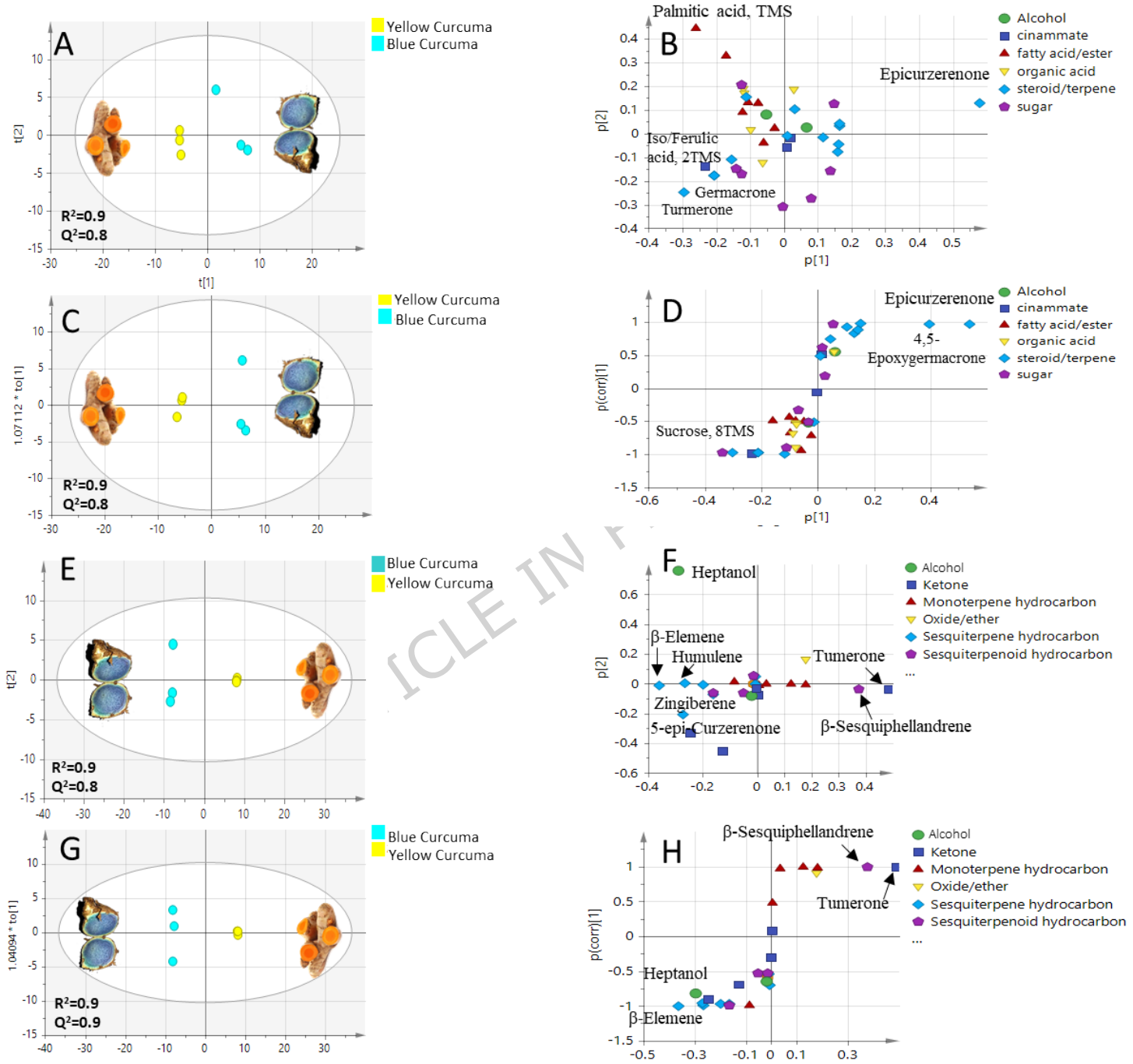

Figure 7: Multivariate data analyses of GC/MS dataset of blue curcuma (*C. caesia*) and yellow curcuma (*C. longa*) of silylated (A-D) and volatile (E-H) components (n=3). Principle component analysis (PCA) score plots (A, E) and loading plots (B, F), orthogonal partial least squares discriminant analysis

(OPLS-DA) score plots (C, G) and S-loading plots (D, H) with PC1 and PC2 represent >70% and > 90% of total variation in data of silylated and volatile components, respectively. Metabolites were assigned based on Mol.wt/Rt as identified in Table 2 and 3.

Table 1: Resonance assignments with chemical shifts of constituents identified in *Curcurma caesia* (blue curcuma) and *Curcurma longa* (yellow curcuma) *via* 600 MHz ^{1}H NMR, HSQC and HMBC spectra.

No	Metabolite	Assignment	^{1}H (multiplicity)	HSQC	HMBC	Blue Curcuma	Yellow Curcuma
1. **Sesquiterpenes**							
1	Curdione	CH_3-13	0.84 d (J = 6.6 Hz)	21.0	C-7 (55.5), C-11 (30.7), C-12 (20.0)	+	-
		CH_3-12	0.94 d (J = 7.0 Hz)	20.0	C-7 (55.5), C-11 (30.7), C-13 (21.0)		
		CH_3-14	0.94 d (J = 6.5 Hz)	18.8	C-3 (35.0), C-4 (47.0), C-5 (216.6)		
2	Xanthorrhizol	CH_3-9	1.17 d (J = 3.0 Hz)	22.1	C-5 (146.5), C-8 (43.0) C-10 (34.5)	+	+
		CH_3-14, 15	1.81 s	18.7	C-13 (134.2)		
		CH_3-7	2.07 s	16.4	C-2 (123.2), C-3 (139.5)		
		H-8	2.48 m	39.8			
		H-12	5.34 m	129.1			
3	Furanodienone	H-15	1.26 s	14.0	C-9 (42.1), C-1 (132.2), C-10 (135.9)	+	-
		H-14	1.94 d (J = 1.2 Hz)	17.6	C-5 (133.2), C-4 (147.7) C-3 (41.0)		
		H-13	2.06 s	8.1	C-11 (123.2),		

No	Metabolite	Assignment	^{1}H (multiplicity)	HSQC	HMBC	Blue Curcuma	Yellow Curcuma
					C-12 (139.5)		
		H-1	5.16 dd (J = 5.0, 11.5 Hz)	130.5			
		H-5	5.87 s	131.8	C-6 (192.0), C-3 (41.0), C-14 (17.6)		
4	Curcuzederone	H-13	2.06 s	8.2	C-11 (123.2), C-12 (139.5)	+	+
		H-5	3.74 s	55.1			
		H-12	7.16 s	139.5	C-11 (123.2), C-8 (159.0)		
5	Curcuminol G	H-15	1.09 s	18.5		+	+
		H-14	1.83 s	18.7			
		H-13	1.87 s	10.5	C-11 (136.0), C-12 (180.0)		
2. **Curcuminoids**							
6	Curcumin I	H-4,4`	7.55 d (J = 15.8 Hz)			-	+
		H-6,6`	7.20 d (J = 1.7 Hz)				
		H-10, 10`	7.09 dd (J = 8.6, 1.7 Hz)				
		H-3,3`	6.59 d (J = 15.8 Hz)				
7	Curcumin II	H-4,4`	7.55 d (J = 15.8 Hz)			-	+
		H-6	7.20 d (J = 1.7 Hz)				
		H-6`, 10`	7.47 d (J = 8.6 Hz)				
		H-7`, 9`	6.80 d (J = 8.6 Hz)				
		H-3,3`	6.59 d (J = 15.8 Hz)				
8	Curcumin III	H-4,4`	7.55 d (J = 15.8 Hz)			-	+
		H-6`, 10`	7.47 d (J = 8.6 Hz)				

No	Metabolite	Assignment	^{1}H (multiplicity)	HSQC	HMBC	Blue Curcuma	Yellow Curcuma
		H-6, 10	7.47 d (J = 8.6 Hz)				
		H-7`, 9`, 7, 9	6.79 d (J = 8.6 Hz)				
		H-3,3`	6.59 d (J = 15.8 Hz)				
3. Primary Metabolites							
9	Methionine	S-CH_3	2.07 s	17.5	CH_2 (29.9)	+	+
		NH_2-CH	3.30 m	48.5			
10	Choline	N(CH_3)$_3$	3.18 s	47.5		+	+
11	Fumaric acid	CH=CH	6.64 br s	134.2		+	+

Table 2: Metabolites profiling of *Curcuma caesia* (blue curcuma) and *Curcuma longa* (yellow curcuma) rhizome methanol extracts *via* UPLC/HR-MS/MS analysis in both negative and positive ionization modes

Peak	Rt (min.)	Identification	Molecular ion $[M-H]^-$ /$[M+H]^+$	Elemental composition	Error (ppm)	Fragments MS^n ion	Blue Curcuma	Yellow Curcuma
I- Sugars								
1	0.59	Hexose	179.0547	$C_6H_{11}O_6^-$	1.6	161, 135, 99, 87, 71, 59	(+)	(+)
2	0.66	Lactobionic acid	357.1030	$C_{12}H_{21}O_{12}^-$	0.7	339, 177, 119, 101, 89, 87, 71, 59	(+)	(+)
3	0.68	Dihexosyl-*O*-glycerol	415.1444	$C_{15}H_{27}O_{13}^-$	0.4	341, 235, 179, 161, 101, 89, 71	(+)	
4	0.69	Trihexoside	503.1614	$C_{18}H_{31}O_{16}^-$	1.5	341, 179, 161	(+)	
5	0.7	Dihexoside	341.1082	$C_{12}H_{21}O_{11}^-$	1.1	179, 161, 101, 89, 71	(+)	(+)
6	0.71	Sugar derivative	267.0712	$C_9H_{15}O_9^-$	0.8	249, 237, 219, 150, 125, 113, 101, 89, 71, 59	(+)	(+)
7	1	Dipentoside	281.0875	$C_{10}H_{17}O_9^-$	2	113, 96, 87, 85, 71, 59	(+)	
II- Organic acids								
8	0.9	Malic acid	133.0128	$C_4H_5O_5^-$	1.9	115, 71	(+)	(+)
9	0.96	Citric acid	191.0188	$C_6H_7O_7^-$	0.9	173, 129, 111, 103, 87	(+)	(+)
10	1.58	Succinic acid	117.0179	$C_4H_5O_4^-$	2.6	99, 73, 55	(+)	
11	1.7	Benzoic acid	121.0280	$C_7H_5O_2^-$	2.5	108, 101, 93, 91	(+)	
III- Phenolics								
12	1.6	Salicylic acid	137.0229	$C_7H_5O_3^-$	2	101, 93, 87, 66	(+)	
13	3.1	Gallic acid-*O*-hexoside	331.0663	$C_{13}H_{15}O_{10}^-$	1.1	315, 168, 150, 125, 89	(+)	
14	3.2	Hydroxy-methoxyphenyl-*O*-hexoside	301.0920	$C_{13}H_{17}O_8^-$	0.8	138, 123, 97	(+)	
15	3.53	Protocatechuic acid-*O*-hexoside	315.0715	$C_{13}H_{15}O_9^-$	1.1	153, 135, 108, 91	(+)	

Table 2: Metabolites profiling of *Curcuma caesia* (blue curcuma) and *Curcuma longa* (yellow curcuma) rhizome methanol extracts *via* UPLC/HR-MS/MS analysis in both negative and positive ionization modes

Peak	Rt (min.)	Identification	Molecular ion $[M-H]^-$ /$[M+H]^+$	Elemental composition	Error (ppm)	Fragments MS^n ion	Blue Curcuma	Yellow Curcuma
16	3.7	Hydroxy-dimethoxyphenyl-*O*-hexoside = (Dimethoxy-hydroquinone-*O*-hexoside) = Leonuriside A	331.1027	$C_{14}H_{19}O_9^-$	0.4	168, 153, 138, 125, 97, 93, 83, 71, 59	(+)	
17	3.72	Protocatechuic acid	153.0183	$C_7H_5O_4^-$	0.4	135, 108, 91	(+)	(+)
18	4	Salicin	285.0973	$C_{13}H_{17}O_7^-$	1.5	267, 195, 177, 123	(+)	
19	4.06	Hydroxyphenyl propanoic acid-*O*-hexoside	343.1028	$C_{15}H_{19}O_9^-$	1.3	181, 163, 137, 119, 101, 89, 71	(+)	
20	4.08	Syringic acid-*O*-hexoside	359.0977	$C_{15}H_{19}O_{10}^-$	1.3	197, 182, 167, 153, 138, 123, 71	(+)	(+)
21	4.7	Eugenol-O-hexoside	325.1284	$C_{16}H_{21}O_7^-$	0.7	163	(+)	(+)
IV- Flavonoids/anthocyanins								
22	4.6	Epi/Catechin	289.0710	$C_{15}H_{13}O_6^-$	1.4	245, 205, 151	(+)	(+)
23	5.65	Malvidin-*O*-rutinoside	639.1912	$C_{29}H_{35}O_{16}^+$	1	493, 331, 150	(+)	
24	5.7	Quercetin-*O*-dirhamnoside	593.1498	$C_{27}H_{29}O_{15}^-$	0.4	300		(+)
25	6.88	Di-*O*-methyl-epi/catechin-*O*-hexoside	479.1552	$C_{23}H_{27}O_{11}^-$	0.48	317, 285, 255, 151, 131	(+)	
26	10.3	Naringenin	271.0606	$C_{15}H_{11}O_5^-$	1.6	253, 177, 151	(+)	
27	12.7	Pinocembrin	255.0654	$C_{15}H_{11}O_4^-$	1.07	213, 151		(+)
V- Cinnamates								
28	3.95	Hydroxy-ferulic acid-*O*-hexoside	373.1131	$C_{16}H_{21}O_{10}^-$	0.5	211, 193, 165, 149, 123, 105, 73	(+)	
29	4.85	Caffeic acid	179.0335	$C_9H_7O_4^-$	2	135	(+)	(+)

Table 2: Metabolites profiling of *Curcuma caesia* (blue curcuma) and *Curcuma longa* (yellow curcuma) rhizome methanol extracts *via* UPLC/HR-MS/MS analysis in both negative and positive ionization modes

Peak	Rt (min.)	Identification	Molecular ion $[M-H]^-$ /$[M+H]^+$	Elemental composition	Error (ppm)	Fragments MS^n ion	Blue Curcuma	Yellow Curcuma
30	7.3	Cinnamic acid	147.0437	$C_9H_7O_2^-$	1	129, 103, 91, 77		(+)
31	8.2	Feruloyloxy-methoxycinnamic acid	339.0862	$C_{19}H_{15}O_6^-$	0.1	193		(+)
32	13.35	Methylbutenoxy ferulic acid	261.1124	$C_{15}H_{17}O_4^-$	1.1	217, 193, 189, 149, 137, 121, 105, 81, 79, 67	(+)	
VI-Alkaloids								
33	3.72	Dihydroxyquinoline carboxylic acid-*O*-hexoside	366.0824	$C_{16}H_{16}NO_9^-$	0.1	204, 185, 173, 160, 130, 107, 102, 93, 87, 73, 68	(+)	(+)
34	4	Trihydroxyquinoline-2-carboxylic acid-*O*-hexoside	382.0771	$C_{16}H_{16}NO_{10}^-$	0.6	366, 351, 220, 176, 121	(+)	(+)
VII- Di/Aryl alkanoids (Curcuminoids)								
35	9.5	Dihydroxy-(hydroxy-dimethoxyphenyl)-(hydroxy-methoxyphenyl) heptane	405.1879	$C_{22}H_{29}O_7^-$	0.02	390, 349, 192, 179, 165, 151, 135, 125, 109	(+)	(+)
36	9.83	Bis(hydroxyphenyl)-hydroxyheptenone	313.1437	$C_{19}H_{21}O_4^+$	1	207, 189, 163, 149, 119		(+)
37	9.86	Calebin A	385.1274	$C_{21}H_{21}O_7^+$	1.9	193, 191, 177, 161, 149, 145, 133, 97		(+)
38	9.9	(Hydroxyphenyl)-(Dihydroxyphenyl)-heptadiene-dione	323.0916	$C_{19}H_{15}O_5^-$	0.6	217, 189, 174, 161, 146, 133, 119, 109, 59		(+)
39	10.32	Curcumalongin A	353.1015	$C_{20}H_{17}O_6^+$	1.5	338, 321, 293, 269, 171, 153, 147		(+)
40	10.35	Hexahydrocurcumin	373.1647	$C_{21}H_{25}O_6^-$	0.5	193, 179, 165, 121	(+)	

Table 2: Metabolites profiling of *Curcuma caesia* (blue curcuma) and *Curcuma longa* (yellow curcuma) rhizome methanol extracts *via* UPLC/HR-MS/MS analysis in both negative and positive ionization modes

Peak	Rt (min.)	Identification	Molecular ion $[M-H]^-$ /$[M+H]^+$	Elemental composition	Error (ppm)	Fragments MS^n ion	Blue Curcuma	Yellow Curcuma
41	10.48	(Dihydroxybenzylidene)-(hydroxy-methoxystyryl) furanone	353.1016	$C_{20}H_{17}O_6^+$	0.8	338, 337, 177, 153, 150, 123		(+)
42	10.6	Curcumalongin B	383.1117	$C_{21}H_{19}O_7^+$	1.8	368, 350, 294, 177, 153, 145, 121		(+)
43	10.7	Curcumalongin C	385.1274	$C_{21}H_{21}O_7^+$	1.8	269, 219, 195, 193, 177, 161, 153, 145, 133, 117		(+)
44	10.91	(Hydroxy-methoxyphenyl)-(hydroxyphenyl)-hydroxyheptadieneone	339.1230	$C_{20}H_{19}O_5^-$	1	219, 189, 175, 161, 149, 134, 119, 69		(+)
45	11.45	Curcolone	245.1174	$C_{15}H_{17}O_3^-$	1	227, 203, 161	(+)	(+)
46	11.48	Tetrahydrodemethoxycurcumin	341.1384	$C_{20}H_{21}O_5^-$	0.4	235, 205, 193, 179, 163, 135, 99	(+)	(+)
47	11.5	Tetrahydrocurcumin	371.1491	$C_{21}H_{23}O_6^-$	0.5	235, 193, 178, 135, 99	(+)	(+)
48	11.7	(Hydroxy-methoxybenzylidene)-(hydroxystyryl) furanone	337.1073	$C_{20}H_{17}O_5^+$	1	321, 305, 160, 147, 137, 123		(+)
49	12.4	Bis(hydroxy-methoxyphenyl)-heptatrien-3-one	353.1378	$C_{21}H_{21}O_5^+$	1.4	285, 259, 225, 197, 177, 161, 145, 137		(+)
50	12.84	Dihydrobisdemethoxycurcumin	309.1124	$C_{19}H_{17}O_4^-$	0.85	203, 189, 161, 145, 119, 93		(+)
51	12.88	Curcumin III, (Bisdemethoxycurcumin)	309.1116	$C_{19}H_{17}O_4^-$	1.9	189, 147, 131, 119		(+)
52	12.95	Bis(dimethoxyphenyl)-pentadienone	355.1532	$C_{21}H_{23}O_5^+$	2	265, 219, 201, 179, 177, 163, 145, 137	(+)	
53	13.05	Curcumin II (Demethoxycurumin)	339.1221	$C_{20}H_{19}O_5^+$	1.7	269, 255, 223, 195, 177, 147, 119	(+)	(+)

Table 2: Metabolites profiling of *Curcuma caesia* (blue curcuma) and *Curcuma longa* (yellow curcuma) rhizome methanol extracts *via* UPLC/HR-MS/MS analysis in both negative and positive ionization modes

Peak	Rt (min.)	Identification	Molecular ion $[M-H]^-$ /$[M+H]^+$	Elemental composition	Error (ppm)	Fragments MS^n ion	Blue Curcuma	Yellow Curcuma
54	13.1	Curcumin I	369.1326	$C_{21}H_{21}O_6^+$	0.4	217, 177, 161, 145, 137, 117	(+)	(+)
55	13.25	Methoxycurcumin	397.1281	$C_{22}H_{21}O_7^-$	0.9	247, 217, 203, 179, 173, 158, 149, 134		(+)
56	14.53	ar-Turmerone	217.1579	$C_{15}H_{21}O^+$	3	119, 103, 91		(+)
57	14.9	Dihydro-ar-Turmerone	219.174	$C_{15}H_{23}O^+$	2.5	121, 105, 93, 83, 79, 55		(+)
VIII- Sesquiterpenes								
58	3.8	Dihydro zedoarolide B-*O*-hexoside	445.2061	$C_{21}H_{33}O_{10}^-$	0.6	283, 265, 247, 239, 221, 219, 203, 185, 167, 161, 151, 133, 111, 71	(+)	
59	4.16	Trihydroxy-guaianenone	429.2141	$C_{21}H_{33}O_9^-$	1.04	411, 393, 267, 249, 231, 179, 161, 142, 139, 119, 89, 71	(+)	
60	4.3	Dihydro derivative of Zedoarolide A	297.1331	$C_{15}H_{21}O_6^-$	0.1	279, 261, 235, 207, 199, 165, 127, 83	(+)	
61	4.4	Zedoarolide B-*O*-hexoside	443.1911	$C_{21}H_{31}O_{10}^-$	0.03	281, 263, 249, 237, 223, 219, 179, 161, 89, 71	(+)	
62	4.8	Zedoalactone A/C/E-*O*-hexoside	427.1966	$C_{21}H_{31}O_9^-$	0.1	265, 247, 235, 207, 189, 161	(+)	
63	5.02	Zedoarolide A	295.1178	$C_{15}H_{19}O_6^-$	0.7	277, 259, 233, 215, 153, 125	(+)	
64	5.05	Hydroxy-(hydroxymethyl)-dimethyl-tetrahydroazulenofuranone (wenyujinin F)	261.1126	$C_{15}H_{17}O_4^-$	1.8	219, 217, 201, 199, 191, 175, 163, 159, 135, 123, 109, 95, 85, 65, 57	(+)	
65	5.07	Zedoalactone B/D	279.1229	$C_{15}H_{19}O_5^-$	0.7	261, 243, 235, 217, 199, 177, 163, 153, 137, 109, 95	(+)	(+)
66	5.8	Zedoarolide B	281.1387	$C_{15}H_{21}O_5^-$	1.4	263, 250, 237, 219, 207, 201, 189, 171, 139, 123, 83	(+)	(+)

Table 2: Metabolites profiling of *Curcuma caesia* (blue curcuma) and *Curcuma longa* (yellow curcuma) rhizome methanol extracts *via* UPLC/HR-MS/MS analysis in both negative and positive ionization modes

Peak	Rt (min.)	Identification	Molecular ion $[M-H]^-$ /$[M+H]^+$	Elemental composition	Error (ppm)	Fragments MS^n ion	Blue Curcuma	Yellow Curcuma
67	6.9	Aerugidiol-*O*-hexoside	411.2014	$C_{21}H_{31}O_8^-$	0.1	249, 231, 213, 191, 179, 161,	(+)	
68	7.1	Unknown sesquiterpene lactone	277.1074	$C_{15}H_{17}O_5^-$	1.4	247, 233, 203, 185, 177, 161, 145, 133	(+)	
69	8	Dihydro derivative of Zedoarolide B	283.1543	$C_{15}H_{23}O_5^-$	1.05	265, 239, 221, 219, 203, 185, 167, 151, 133	(+)	
70	11.3	Hexahydro-dihydroxy-trimethylazulenofuranone (wenyujinolides A/B)	263.1281	$C_{15}H_{19}O_4^-$	1.4	245, 201, 219, 191, 149,137, 125, 109, 97	(+)	
71	12.5	Zedoalactone A/C/E	265.1452	$C_{15}H_{21}O_4^-$	0.2	221, 191, 147	(+)	
72	12.9	Germacrone epoxide	235.1685	$C_{15}H_{23}O_2^+$	2	217, 207, 193, 189, 175, 161, 147, 135, 119, 107, 105, 93, 79, 69, 67	(+)	
73	12.97	Furandiene	217.1585	$C_{15}H_{21}O^+$	0.8	199, 189, 175, 161, 135, 119, 107, 105, 93, 79, 69	(+)	
74	13	Confertin	247.1330	$C_{15}H_{19}O_3^-$	0.1	221, 203, 178, 149, 135, 111, 95, 57	(+)	
75	13.02	Curcumenol	235.1685	$C_{15}H_{23}O_2^+$	2.3	217, 199, 189, 179, 177, 161, 149, 121, 119, 113, 107, 105, 97, 95, 93, 85, 79, 69, 65, 55	(+)	(+)
76	13.14	Curcumenone	235.16878	$C_{15}H_{23}O_2^+$	0.4	207, 189, 165, 151, 149, 123, 119, 107, 83, 71	(+)	
77	13.32	Zederone	247.1319	$C_{15}H_{19}O_3^+$	3	229, 201, 183, 139, 123, 121, 107, 95, 81, 67, 65	(+)	(+)
78	13.7	Curdione	237.1843	$C_{15}H_{25}O_2^+$	2.3	221, 219, 201, 191, 135, 121, 109, 107, 93, 81, 69, 55	(+)	(+)

Table 2: Metabolites profiling of *Curcuma caesia* (blue curcuma) and *Curcuma longa* (yellow curcuma) rhizome methanol extracts *via* UPLC/HR-MS/MS analysis in both negative and positive ionization modes

Peak	Rt (min.)	Identification	Molecular ion $[M-H]^-$ /$[M+H]^+$	Elemental composition	Error (ppm)	Fragments MS^n ion	Blue Curcuma	Yellow Curcuma
79	13.76	Germacrone/Zerumbone	219.1739	$C_{15}H_{23}O^+$	1.9	203, 159, 135, 121, 107, 97, 93, 79, 69	(+)	(+)
80	14	Aerugidiol	249.1493	$C_{15}H_{21}O_3^-$	3	231, 223, 213, 205, 189, 184, 177, 165, 147, 113, 87, 79.9, 68, 55	(+)	(+)
81	14.14	Epi/Curzerenone	231.1374	$C_{15}H_{19}O_2^+$	2.1	213, 203, 198, 189, 183, 173, 161, 149, 135, 119, 105, 95, 83	(+)	
IX- Fatty acids/esters								
82	6.61	Suberic acid	173.0806	$C_8H_{13}O_4^-$	0.8	129, 111, 83, 67, 57	(+)	(+)
83	7.99	Azelaic acid	187.0963	$C_9H_{15}O_4^-$	0.6	169, 143, 125		(+)
84	11.4	Trihydroxyoctadecenoic	329.2327	$C_{18}H_{33}O_5^-$	1.4	229, 211, 183, 171	(+)	
85	12.8	Trihydroxyoctadecanoic acid	331.2482	$C_{18}H_{35}O_5^-$	1	313, 295, 277, 185, 127		(+)
86	13.3	Gingerglycolipid A	675.3589	$C_{33}H_{55}O_{14}^-$	0.4	415, 397, 277, 255, 235, 161, 101	(+)	
87	13.34	Dihydroxyoctadecadienoic acid	311.2219	$C_{18}H_{31}O_4^-$	0.9	293, 275, 249, 183, 171	(+)	
88	13.4	Hydroxy-oxopentadecanoic acid	271.1908	$C_{15}H_{27}O_4^-$	1.7	253, 227, 209, 97	(+)	(+)
89	13.56	Hydroxy-oxopentadecadienoic acid	267.1594	$C_{15}H_{23}O_4^-$	1.4	249, 223, 205, 197, 181, 137, 97, 85	(+)	
90	13.79	Hydroxy-oxohexadecanoic acid	285.2064	$C_{16}H_{29}O_4^-$	1.3	267, 223, 59		(+)
91	14.1	Glyceropalmitoyl-*O*-dihexoside	653.3743	$C_{31}H_{57}O_{14}^-$	0.07	415, 397, 323, 255, 179, 89	(+)	
92	14.18	Palmitoyl-sn-glycero-phosphoethanolamine (LysoPE(0:0/16:0)	452.2775	$C_{21}H_{43}NO_7P^-$	0.8	339, 255, 196	(+)	

Table 2: Metabolites profiling of *Curcuma caesia* (blue curcuma) and *Curcuma longa* (yellow curcuma) rhizome methanol extracts *via* UPLC/HR-MS/MS analysis in both negative and positive ionization modes

Peak	Rt (min.)	Identification	Molecular ion $[M-H]^-$ /$[M+H]^+$	Elemental composition	Error (ppm)	Fragments MS^n ion	Blue Curcuma	Yellow Curcuma
93	14.2	Oleoyl glycero-phosphoethanolamine	478.2931	$C_{23}H_{45}NO_7P^-$	0.7	339, 281, 196	(+)	
94	14.23	Hydroxy octadecadienoic acid	295.2271	$C_{18}H_{31}O_3^-$	1.2	277, 195	(+)	(+)
95	15	Hydroxypalmitic acid	271.2270	$C_{16}H_{31}O_3^-$	1	253, 225		(+)
96	17	Oleoyl-*O*-methyl-glycero-phosphate	449.2666	$C_{22}H_{42}O_7P^-$	0.8	281, 167	(+)	
97	17.02	Dilinoleoyl-glycero-phosphate	695.4646	$C_{39}H_{68}O_8P^-$	0.04	415, 279, 153	(+)	
98	17.04	Palmitoyl-linoleoyl-glycero-phosphoinositol	833.5173	$C_{43}H_{78}O_{13}P^-$	0.15	553, 391, 279, 255	(+)	(+)
99	17.06	Dioleoylglycerophosphate	697.4793	$C_{39}H_{69}O_8P^-$	0.53	415, 280	(+)	(+)
100	17.07	Linoleoyl-glycerophosphate	433.2352	$C_{21}H_{38}O_7P^-$	0.6	279, 153	(+)	
101	17.1	Palmitoyl-linoleoyl-glycero-phosphate	671.4642	$C_{37}H_{68}O_8P^-$	0.5	415, 391, 279, 255	(+)	(+)
102	17.2	Palmitoyl-oleoyl-glycerophosphoinositol	835.5312	$C_{43}H_{80}O_{13}P^-$	2	553, 281, 255	(+)	(+)
X- Miscellaneous								
103	1.1	Uridine	243.0614	$C_9H_{11}O_6N_2^-$	0.9	183, 153, 140, 113, 110	(+)	
104	3.12	Methyl Uridine	257.0772	$C_{10}H_{13}O_6N_2^-$	1.6	228, 214, 183, 155, 139, 124, 109	(+)	
105	3.59	Panthenol	204.1227	$C_9H_{18}NO_4^-$	1.6	125, 102, 71, 59	(+)	
106	3.71	Pyroglutamic acid	128.0339	$C_5H_6NO_3^-$	2	98, 81, 65	(+)	
107	4.1	Unknown	271.1181	$C_{13}H_{19}O_6^-$	1.7	193, 177, 135	(+)	(+)
108	4.9	Unknown	425.2019	$C_{18}H_{33}O_{11}^-$	0.5	293, 263, 209	(+)	

Table 2: Metabolites profiling of *Curcuma caesia* (blue curcuma) and *Curcuma longa* (yellow curcuma) rhizome methanol extracts *via* UPLC/HR-MS/MS analysis in both negative and positive ionization modes

Peak	Rt (min.)	Identification	Molecular ion $[M-H]^-$ /$[M+H]^+$	Elemental composition	Error (ppm)	Fragments MS^n ion	Blue Curcuma	Yellow Curcuma
109	5.81	Hydroxy-trimethyl-cyclohexenoic acid-O-hexoside (picrocrocinic acid)	345.1547	$C_{16}H_{25}O_8^-$	1.03	179, 165, 161, 149, 137, 123, 101, 89		(+)
110	5.82	Dihydroxy-megastigmadien-one-*O*-hexoside (blumenol hexoside)	385.1866	$C_{19}H_{29}O_8^-$	2.4	223, 205, 161, 153, 101		(+)

Table 3: Relative percentiles of silylated compounds detected in *C. caesia* and *C. longa via* GC/MS analysis

Peak	Rt (min.)	KI	Identification	*C. longa*	*C. caesia*
Sugars					
1	14.9	1814.5	D-Fructose, 5TMS *	0.02 ± 0.003	0.05 ± 0.03
2	15.3	1854	Methyl .alpha.-Arabinofuranoside, 3TMS	0.09 ± 0.05	0.32 ± 0.04
3	15.90	1904.7	Glucose, 5TMS *	5.59 ± 0.44	5.86 ± 1.09
4	16.1	1915	Methyl pentopyranoside	2.27 ± 0.23	1.21 ± 0.33
5	16.7	1989.8	b-Glucopyranose, 5TMS	0.53 ± 0.05	0.35 ± 0.26
6	16.7	1989	Talose, 5TMS	11.97 ± 1.15	10.98 ± 2.35
7	22.4	2674	Sucrose, 8TMS *	20.02 ± 1.15	11.16 ± 1.56
Total sugars				**40.5**	**29.93**
Organic acids					
8	13.6	1690	2-Methyl-2-butenedioic acid dimethyl ester	2.63 ± 0.2	1.78 ± 1.22
9	5.15	1063.1	Lactic Acid, 2TMS*	1.72 ± 0.71	0.84 ± 0.27
10	7.87	1237.4	Benzoic Acid, TMS	0.14 ± 0.01	0.57 ± 0.54
11	11.2	1487.5	Malic acid, 3TMS	1.37 ± 0.04	0.86 ± 0.21
12	13.09	1641	Glutaric acid, di(isobutyl) ester	2.35 ± 0.13	1.56 ± 1.06
Total organic acids				**8.2**	**5.61**
Alcohols					
13	8.3	1272.1	Glycerol, 3TMS *	1.79 ± 0.12	2.36 ± 0.67
14	12.0	1553	1-Dodecanol, TMS	0.45 ± 0.04	0.28 ± 0.24
Total Alcohols				**2.24**	**2.64**
Cinnamates					
15	14.3	1751	Hydrocinnamic acid 2TMS	0.09 ± 0.005	0.11 ± 0.03
16	16.1	1929	4-Coumaric acid, 2TMS	0.16 ± 0.03	0.15 ± 0.09
17	17.6	2082	(Iso)ferulic acid, 2TMS	4.22 ± 0.42	0.06 ± 0.03
Total cinnamates				**4.47**	**0.32**
Steroid/terpene					
18	11.3	1493.7	Curzerene	0.037 ± 0.01	1.55 ± 0.9

Peak	Rt (min.)	KI	Identification	*C. longa*	*C. caesia*
19	12.6	1599.3	Epicurzerenone	0.09 ± 0.02	22.29 ± 4.44
20	13.2	1657	aR-Turmerone	7.13 ± 1.9	0.14 ± 0.05
21	13.6	1695	Curlone	3.59 ± 0.84	0.21 ± 0.04
22	13.7	1698.1	Germacrone	3.59 ± 0.84	0.21 ± 0.04
23	13.9	1718	Neocurdione	0	0.01 ± 0.01
24	14.1	1739	b-Eudesmol, TMS	0.17 ± 0.05	1.02 ± 0.3
25	14.3	1718.4	Curdione	0.48 ± 0.04	0.68 ± 0.15
26	15.18	1832.8	Curcumenone	1.25 ± 0.15	0.19 ± 0.03
27	15.3	1845	4,5-Epoxygermacrone	0.16 ± 0.01	12.14 ± 2.49
28	16.8	1994.3	Zederone	0.11 ± 0.07	1.89 ± 0.33
29	17.7	2101.8	Valerenic acid, TMS	0.43 ± 0.14	2.16 ± 0.74
30	28.2	3467	b-Sitosterol, TMS	0.06 ± 0.02	0.04 ± 0.02
Total steroid/terpene				**17.1**	**42.54**
Fatty acids/esters					
31	17.08	2025	Palmitic Acid, TMS *	14.21 ± 1.16	10.24 ± 6.1
32	18.6	2190	Linoleic acid, TMS	1.11 ± 0.04	0.82 ± 0.07
33	18.6	2201.8	Oleic Acid, (Z)-, TMS	0.15 ± 0.01	0.1 ± 0.04
34	18.71	2201.9	11-Octadecenoic acid, (Z)-, TMS	1.11 ± 0.11	0.77 ± 0.5
35	18.8	2219	Stearic acid, TMS	6.4 ± 0.59	4.68 ± 3.05
36	21.7	2571	1-Monopalmitin, 2TMS	2.42 ± 0.87	1.29 ± 0.53
37	22.9	2571	1-Monolinolein, 2TMS	0.18 ± 0.01	0.12 ± 0.04
38	23.13	2763	Glycerol monostearate, 2TMS	1.92 ± 1.27	0.93 ± 0.64
Total fatty acid/ester				**27.49**	**18.95**

*denotes compounds confirmed using standards